frontiers | Frontiers in Marine Science

TYPE Original Research
PUBLISHED 12 April 2023
DOI 10.3389/fmars.2023.1093982

OPEN ACCESS

EDITED BY
Gui Manuel Machado Menezes,
University of the Azores, Portugal

REVIEWED BY
Angelo Bonanno,
National Research Council (CNR), Italy
Ben Scoulding,
Commonwealth Scientific and Industrial Research Organisation, Australia

*CORRESPONDENCE
Airam N. Sarmiento-Lezcano
sarmientolez@gmail.com;
airam.sarmiento@ulpgc.es

SPECIALTY SECTION
This article was submitted to Deep-Sea Environments and Ecology, a section of the journal Frontiers in Marine Science

RECEIVED 09 November 2022
ACCEPTED 21 March 2023
PUBLISHED 12 April 2023

CITATION
Sarmiento-Lezcano AN, Olivar MP, Caballero MJ, Couret M, Hernández-León S, Castellón A and Peña M (2023) Swimbladder properties of *Cyclothone* spp. in the northeast Atlantic Ocean and the Western Mediterranean Sea. *Front. Mar. Sci.* 10:1093982. doi: 10.3389/fmars.2023.1093982

Swimbladder properties of *Cyclothone* spp. in the northeast Atlantic Ocean and the Western Mediterranean Sea

Airam N. Sarmiento-Lezcano[1]*, M. Pilar Olivar[2], María José Caballero[3], María Couret[1], Santiago Hernández-León[1], Arturo Castellón[4] and Marian Peña[5]

[1]Instituto de Oceanografía y Cambio Global, Universidad de Las Palmas de Gran Canaria, Unidad Asociada ULPGC-CSIC, Gran Canaria, Canary Islands, Spain, [2]Institut de Ciències del Mar (ICM), Consejo Superior de Investigaciones Científicas (CSIC), Barcelona, Spain, [3]Division of Veterinary Histology and Pathology, Institute for Animal Health and Food Safety (IUSA), Veterinary School, University of Las Palmas de Gran Canaria, Arucas, Spain, [4]Unidad de Tecnología Marina (UTM), Consejo Superior de Investigaciones Científicas (CSIC), Barcelona, Spain, [5]Centro Oceanográfico de Baleares (Instituto Español de Oceanografía (IEO), Consejo Superior de Investigaciones Científicas (CSIC), Palma, Spain

Non-migratory bristlemouth fishes (*Cyclothone* spp.) are the most abundant vertebrates on Earth and play an important role in the biological carbon pump by remineralizing organic carbon in deep ecosystems. Acoustic data and net sampling are often used in combination to estimate fish and zooplankton biomass, but this procedure may be subject to several sources of error when applied to mesopelagic species. For instance, the allocation of echoes to species has often been biased by not considering *Cyclothone* spp. due to the use of nets targeting larger fish. Furthermore, the acoustic properties of the target organisms must be well understood to convert acoustic density into numerical density. The characteristics of a fish's swimbladder are the most relevant features necessary to assess its acoustic properties. This study provides information on the swimbladder properties of six *Cyclothone* species inhabiting the meso- and bathypelagic layers in the North Atlantic Ocean and Mediterranean Sea, including swimbladder location within the body, fat tissue content, morphology, morphometry (only available for *C. braueri* and *C. pseudopallida*), and fish body-mass density (only available for *C. braueri*, *C. pseudopallida*, *C. pallida*, and *C. pygmaea*). The studied species showed a functional physoclistous swimbladder, with well-developed gas glands and rete mirabile and numerous capillaries in the case of the shallower species *C. braueri* and *C. pseudopallida* (mainly distributed from 400 to 600 m depth), and a fat-invested swimbladder in species with deeper vertical distribution (*C. livida*, *C. microdon*, *C. pallida*, and *C. pygmaea*). The fat content in the swimbladder (*C. pallida* and *C. microdon*) increased with depth and latitude, reducing the space in the swimbladder that could contain gas. Changes in swimbladder size and volume during growth were analyzed for shallower species, where swimbladder volume and equivalent radius followed negative allometric growth in relation to body length. Finally, values of body-mass density (ρ) and gas content required for neutral buoyancy (V_G) were estimated for *C. braueri* and *C. pygmaea* collected between 350 and 550 m (ρ = 1.052–1.072 g·cm^{-3}, V_G = 2%–4%; ρ = 1.052–1.062 g·cm^{-3}, V_G =

3.6%), and for *C. pallida* and *C. pseudopallida* sampled in the 450–700 m layer (ρ = 1.052–1.062 g·cm^{-3}, V_G = 2.6–3.1%; ρ = 1.052–1.062 g·cm^{-3}, V_G = 2.8%–3.25%). Results in this study highlight the change in scattering behavior of *Cyclothone* species from gas-bearing organisms (those that contain gas in their swimbladder) in the upper mesopelagic zone to the fluid-like scattering (with fat-filled swimbladders) of the deeper and northern individuals. The data presented in this manuscript are important for parametrizing acoustic backscattering models built to estimate the echo of *Cyclothone* species, although further work is needed, particularly for individuals with partially invested swimbladders with an irregular fat-free shape.

KEYWORDS

micronekton, bristlemouth, swimbladder, gas, fatty-tissue, histology, body-mass density

1 Introduction

The fish biomass in the mesopelagic (200–1,000 m depth) and bathypelagic (1,000–4,000 m depth) zones constitutes a large fraction of the estimated total global fish biomass, particularly in the upper mesopelagic zone (200–600 m depth) where most of the abundance is concentrated (Sarmiento-Lezcano et al., 2022). The lower mesopelagic zone (600–1,000 m depth) and the bathypelagic zone on the other hand are usually inhabited by fewer organisms, although they are generally of larger sizes, increasing the proportional biomass (Badcock, 1970; Badcock and Merrett, 1976; Roe and Badcock, 1984; Olivar et al., 2012; Olivar et al., 2017). These species are the main prey of many large pelagic migrators (Schaber et al., 2022) and are also expected to be harvested for human consumption in the near future as a source of marine fat and protein (e.g., Gjøsaeter and Kawaguchi, 1980; FAO, 1997; FAO, 2001; Hidalgo and Browman, 2019; Grimaldo et al., 2020). Moreover, meso- and bathypelagic fishes contribute to the biological carbon pump, exporting organic carbon from the euphotic zone to the meso- and bathypelagic layers in the case of migratory fish, and remineralizing (breakdown or transformation of organic matter molecules into their simplest inorganic forms) in the case of non-migratory fishes that remain at depth (Lampitt et al., 2008; Guidi et al., 2015; Sarmiento-Lezcano et al., 2022). *Cyclothone* spp., are the most abundant among the non-migratory group (Sarmiento-Lezcano et al., 2022) and the most abundant vertebrates on the planet (Ahlstrom et al., 1984; Nelson et al., (2016) are known to contribute significantly to the non-migrant deep scattering layers detected acoustically (Peña et al., 2014).

Acoustic methodology combined with net trawling is often employed to estimate the abundance of aquatic organisms (Simmonds and MacLennan, 2005). However, an accurate abundance estimate is not yet available for meso- and bathypelagic species due to poor capture efficiency (Koslow et al., 1997; Kloser et al., 2009; Yasuma and Yamamura, 2010; Kaartvedt et al., 2012), vessel and platform avoidance (Peña, 2019; Peña et al., 2020), and acoustic uncertainties (Davison et al., 2015; Peña, 2019; Proud et al., 2019). A global mesopelagic fish biomass estimate using 38 kHz data (11–15 Gt; Irigoien et al., 2014) was an order of magnitude higher than a previous estimate from micronekton nets (1 Gt; Gjøsaeter and Kawaguchi, 1980). However, Irigoien et al. (2014) did not consider the large contribution of *C. braueri* to the most prominent scattering layer at 38 kHz (400–700 m) in many areas of the world (Peña et al., 2014; Ariza et al., 2016; Peña, 2019). Their resonant target strength at those depths and their low individual biomass would considerably reduce the estimated biomass. The acoustic contribution of non-migrating *Cyclothone* spp. to mesopelagic acoustic layers has often been underestimated due to the use of nets targeting larger fishes. However, their abundance often masks the echo of migrating species at 38 kHz (Peña et al., 2020).

The use of several frequencies in acoustics allows classifying areas of the echogram as gas-bearing, fluid-like, or elastic-shelled echotraces (Stanton et al., 1996), employing scattering models and clustering techniques (Peña and Calise, 2016; Peña, 2018; Peña et al., 2023a; Peña et al., 2023b). Scattering models reproduce the expected echo of an organism at different frequencies based on body morphology and behavior (Ona, 1990; Ona, 1999). Acoustic backscatter depends firstly on the existence of a swimbladder or gas enclosure. When gas is present, up to 95% of the acoustic backscatter is due to the swimbladder (Foote, 1980). Swimbladder size and depth in the water column determine both the intensity of the echo and the spectra (trend with frequency; Peña et al., 2014). Other important input parameters for the scattering models are orientation, size, shape, and material properties (density and sound contrast with the surrounding water). Therefore, knowledge of the swimbladder characteristics of the target species is of paramount importance for acoustic data elucidation.

Marshall (1951; 1960) described the swimbladder of several meso- and bathypelagic fishes, showing its structure from larval to adult stages. Larval stages of most mesopelagic fish dwell in the epipelagic layers (Olivar et al., 2018) and have swimbladders containing gas (Marshall, 1951; Marshall, 1960). For some species, such as bristlemouths of the genus *Cyclothone* and some

myctophids, the organ regresses with age and is filled with fat in late adults (Marshall, 1960). Some information on the structures of *Cyclothone* swimbladders (*C. braueri*, *C. signata*, *C. acclinidens*, *C. livida*, and *C. microdon*) was described by Marshall (1960). However, there is little information about other bristlemouth species present in the Atlantic Ocean and the Mediterranean Sea, or on the evolution of swimbladder shape and gas/lipid content with age. The use of terms such as inflated, contracted, or regressed swimbladder without a detailed explanation gives rise to confusion in the literature. In fact, the same species (*C. braueri*) with similar length were described as non-gas-bearing (Kleckner and Gibbs, 1972; Escobar-Flores et al., 2018) or gas-bearing glanding (Marshall, 1979; Peña et al., 2014), highlighting the need for further studies of the swimbladder of these species.

The main swimbladder organs are the gas gland and the *rete mirabile*. The gas gland allows oxygen exchange between the blood and lumen of the gas bladder. The *rete mirabile* (a bundle of closely packed venous and arterial capillaries attached to the gas gland and entering the swimbladder anteriorly) supplies blood to the gas gland and maintains a pressure differential between the blood and gas bladder through a countercurrent system (Marshall, 1960; Denton, 1961; Kuhn et al., 1963). A functional swimbladder has well-developed cells in the gas gland and the *rete mirabile*. On the other hand, non-functional swimbladders present atrophied cells in those areas due to the contraction of the gas gland and *rete mirabile* (Horn, 1975; Neighbors, 1992). Physoclistous fishes (species without a pneumatic duct connecting the swimbladder with the gut) must have a well-developed gas gland and a *rete mirabile* with enough resorptive area to fill and empty the gas bladder through the blood cells.

The aim of the present study was to analyze the swimbladder properties of six bristlemouth species of the genus *Cyclothone* in the meso- and bathypelagic layers of the North Atlantic Ocean and Mediterranean Sea. We analyzed the swimbladder location within the body and its shape, the increase in fat content, and swimbladder degradation with length and body mass density. One of the main objectives was to obtain an indication of swimbladder functionality by species and lengths, that is, the probability of the swimbladder containing gas.

2 Materials and methods

The biological data examined in this study were collected from three research cruises in the Atlantic: *Bathypelagic* (24 May–23 June 2018), from northwest Africa (20°N 20°W), to the south of Iceland (60°N 20°W), *SUMMER* (30 September–18 October 2020), from the western Mediterranean to the Atlantic around the Iberian Peninsula, and *IDEADOS* (12 July–29 July 2010), from the Northwest Mediterranean Sea (40°N 2°E to 40°N 2.45°E) on board the R.V. "Sarmiento de Gamboa" (see Figure 1). Specimens used to examine swimbladders were collected during the *Bathypelagic* and *SUMMER* surveys; those for body-mass density came from the *SUMMER* cruise, while distribution data were obtained on the *Bathypelagic* and *IDEADOS* cruises. Samples were obtained with the "Mesopelagos" midwater trawl net

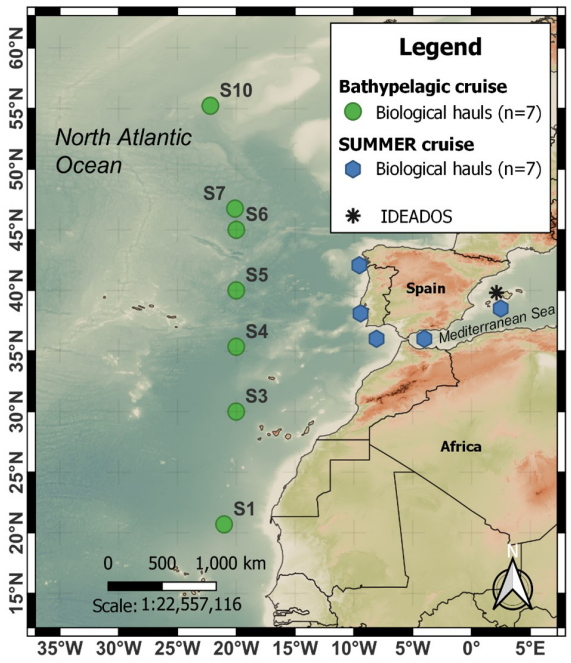

FIGURE 1
Sampling area and location of stations in the northeast Atlantic during the Bathypelagic (green dots) cruise and western Mediterranean during the SUMMER (blue diamonds) and IDEADOS (black asterisks) cruises on board the *R.V. "Sarmiento de Gamboa."*

(Meillat, 2012; Castellón and Olivar, 2023) and MOCNESS-1 m^2 zooplankton net (Wiebe et al., 1985) during day and night hauls carried out from the surface to 700–800 m during the *SUMMER* and *IDEADOS* cruises, and to 1,900 m on the *Bathypelagic* cruise. The Mesopelagos net had an average mouth opening of 29–35 m^2 and a total length of 58 m. The gear consists of graded-mesh netting starting at 30 mm and ending at 4 mm. A multi-sampler (Castellón and Olivar, 2023) was installed at the cod-end to collect samples from five different depth layers. Depth samples on the *Bathypelagic* cruise were obtained from 1,900 to 1,200 m, 1,200 to 800 m, 800 to 500 m, 500 to 200 m, and 200 to 0 m, except for station 7 that only reached 600 m depth (see Sarmiento-Lezcano et al., 2022). For the *SUMMER* cruise, the depth layers were 700–600 m, 600–500 m, 500–400 m, 400–300 m, 300–200 m, 200–100 m, and 100–0 m. On both cruises, the ship speed during the hauls was maintained at 2–2.5 knots. Specimens collected with the Mesopelagos net were immediately identified, measured (standard length, SL), and used for body mass density (ρ) (Table 1).

The MOCNESS-1 m^2 net was fitted with a 0.2 mm mesh size, and the ship speed during deployment and retrieval was maintained between 1.5 and 2.5 knots to obtain a net angle between 40° and 50°, and the winch retrieval rate was fixed at 0.3 m s^{-1} on the *IDEADOS*, *Bathypelagic*, and *SUMMER* cruises (see Olivar et al., 2012 for the *IDEADOS cruise*, Sarmiento-Lezcano et al., 2022 for the *Bathypelagic cruise*, and Olivar et al., 2022 for the *SUMMER cruise*). The sampling layer depths were the same as for the Mesopelagos on the *Bathypelagic* and *SUMMER* cruises (see above), and for *IDEADOS* samples were obtained from 900 to 800 m, 800 to 700 m, 700 to 600 m, 600 to 500 m, 500 to 400 m, 400

TABLE 1 Number of specimens used in histological analysis, morphological, and body-mass density measurements.

Species	Histology **		Morphology **	Body mass density*	
	North Atlantic	Mediterranean Sea	North Atlantic	North Atlantic	Mediterranean Sea
C. braueri	34	46	215	48	35
C. pseudopallida	14		38	15	
C. pygmaea		18			1
C. pallida	55			29	
C. livida	8				
C. microdon	19				

**MOCNESS-1 net (200 µm of mesh size) and the *Mesopelagos net (4 mm of cod-end mesh size).

to 300 m, 300 to 200 m, and 200 to 0 m depths. Biological samples were preserved in 5% buffered formalin, and specimens were sorted out and measured later in the laboratory. Shrinkage correction for formalin preservation was not applied because all our specimens were transformations, juveniles (>12 mm of SL, see Olivar et al., 2018), or adults (according to fish length at 50% maturity (L_{50}); Miya and Nemoto, 1986; McKelvie, 1989; Miya and Nemoto, 1991), and shrinkage in pelagic fishes is negligible at those developmental stages where the degree of ossification is high (Theilacker, 1980). Samples from this net were used for histology and morphology.

Individuals collected during the *Bathypelagic* cruise were used to measure the sizes of individuals and the morphological swimbladder measurements. Body-mass density (ρ) and histology examinations were carried out on fish collected during the *SUMMER* cruise (Table 1). Information on distribution, abundance, and size frequency distributions was gathered from the *Bathypelagic* and *IDEADOS* cruises. The abundances within each layer of the water column are given as the number of individuals per 1,000 m^{-3} of water filtered by the net in each sampled layer.

2.1 Standard length distribution

Size-frequency distributions of *Cyclothone* spp. were calculated from the MOCNESS-1 to determine the predominant size classes during diurnal and nocturnal periods. For this analysis, abundances in 5 mm interval size classes were estimated. *Cyclothone* species were classified into shallower species (*C. braueri* and *C. pseudopallida*) and deeper species (*C. pygmaea*, *C. pallida*, *C. livida*, and *C. microdon*) according to their vertical distribution in the water column. Both groups were differentiated according to the weighted mean depth (WDM) for each species, estimated as follows:

$$WMD = \frac{\sum_{i=1}^{n}(WD_i \star A_i)}{\sum_{i=1}^{n} A_i}$$

where. WD_i. is the mean sampling depth of the *i*th depth stratum, and A_i is the abundance (Ind/1,000 m^3) or biomass (dry weight/1,000 m^3) of each species in the *i*th depth stratum. The Pearson correlation coefficient (r) was used to evaluate the linear correlation between depth and standard length.

2.2 Histological analysis

A total of 175 individuals from six species were examined by histological analysis to obtain a detailed description of the swimbladder location in the body and to determine the evolution of fat-tissue content with length (Table 2). All fish formalin-fixed tissues were dehydrated, cleared, and embedded in paraffin. Organisms were longitudinally sectioned at 4 µm and stained with hematoxylin and eosin. Between six and 10 sections equally spaced (depending on the organism's thickness), were made from each sample, and the section with the largest swimbladder area was used. The slides were examined with a light microscope (Olympus BX51TF, Japan). The proportion of the swimbladder area occupied by fat was calculated using ImageJ (Schneider et al., 2012). Measurements of the gas gland, *rete mirabile* area, area and number of cells, and diameter of capillaries at different lengths were made to infer whether the swimbladder was functional as a proxy for gas content (see Table 3). The percentage of area with fat tissue (%FT) in *Cyclothone* spp. swimbladders was linearly regressed against standard length (mm) (Table 4). The maximum percentage area with gas (%GAS), that is, the area with no fat that could be filled with gas, was then estimated as 100-%FT, and the spatial (vertical and horizontal) distributions of standard-length distributions were transformed into vertical and geographical distributions of %GAS weighted by abundance and biomass.

2.3 Swimbladder measurements of semi-transparent species

Swimbladders of shallow species (*C. braueri* and *C. pseudopallida*), characterized by light pigmentation and semi-transparent swimbladders, were measured using a stereomicroscope. A selection of specimens with gas-filled swimbladders from those examined through histology was used to

10.3389/fmars.2023.1093982

TABLE 2 Summary of *Cyclothone* spp. examined with histology.

Species	Haul depth range (m)	SL (mm)	Ww (mg)	% FT	N
C. braueri	300–400	22 ± 2.3	46.9 ± 14.4	–	22
C. braueri	400–500	18.8 ± 2.4	27.9 ± 12.6	–	38
C. braueri	500–600	22 ± 2.9	48 ± 15.8	–	16
C. braueri	0–700	21.7 ± 1.7	45.3 ± 10.1	–	4
C. pseudopallida	600–700	24.6 ± 5.6	33.5 ± 15.1	–	11
C. pseudopallida	0–700	28.3 ± 1.1	42.3 ± 3.4	–	3
C. pygmaea	600–700	22.4 ± 2.2	41.84 ± 12.8	78.53 ± 2.28	18
C. pallida	600–700	27.9 ± 5.1	64.3 ± 29.3	81.91 ± 15.75	32
C. pallida	0–700	29.4 ± 8.5	76.5 ± 39.9	83.67 ± 6.65	23
C. livida	0–700	33.5 ± 11.8	168.9 ± 142.9	76.74 ± 4.22	8
C. microdon	700–1,000	33.5 ±2.3	147.8 ± 29.8	85.8 ± 22.05	8
C. microdon	1,000–1,300	31.6 ± 1.4	122.1 ± 17.6	82.45 ± 3.46	8
C. microdon	1,600–1,900	36.3 ± 6.3	201.8 ± 95.1	92.3 ± 2.46	3

SL, body fish standard length; Ww, fish wet weight; %FT, percentage of area with fat tissue; N, number of individuals.

take morphometric measurements of the swimbladders. A total of 253 specimens (see Table 1 for number and species taken for morphology) were photographed with a camera (Leica DFC450) mounted on a stereo microscope (Leica M205C) to obtain swimbladder length (SwL), height (SwH), width (SwW), and swimbladder angle (Swθ) (Figure 2). The longitudinal axis of the fish body was set as the reference line for the angle (θ = 0), with positive values over the reference line. Swimbladder measurements were taken with an ocular micrometer to the nearest 0.1 mm. Swimbladder allometric growth with respect to the standard length was estimated following Osse and van den Boogaart (2004) and Yasuma et al. (2010) using a potential relationship $Sw_i = p * SL^q$, where Sw_i is the swimbladder measure, p is the intercept of the regression model, and q is the slope (or allometric coefficient). For length relationships among SwL, SwH, SwW, and Swθ versus SL, the allometric coefficient of 1 indicates isometry, i.e., swimbladder growth and stand length are proportional. If the growth model is negatively allometric, the body grows relatively faster than the swimbladder. However, isometry is different for the swimbladder area (an allometric coefficient of 2) and volume (an allometric coefficient of 3). Swimbladder volumes were approximated using the formula for a prolate spheroid: $V = 4/3\ \pi ab^2$, where a (*SwL/2*) and b (*SwH/2*) are the major and minor semiaxes, respectively (Capen, 1967). The equivalent spherical radius (*ESR*) was estimated following

TABLE 3 Size characteristics of gas gland and rete mirabile in four species of *Cyclothone* (Figures 7A, B).

Species	Depth (m)	SL (mm)	Gas gland		Rete mirabile			
			Area (mm^2)	Cell area (μm^2)	Area (mm^2)	Capi. diam. (μm)	N. capi. measured	N. capi. observed
C. braueri	400–500	20	0.026	303–957	0.004	3–10	9	35
C. braueri	400–500	20	0.021	520–2,000	0.003	2–7	7	36
C. pseudopallida	600–700	19	2.21	1,000–3,400	0.05	3–10	12	32
C. pseudopallida	600–700	25	0.019	118–603	0.015	4–8	20	27
C. pallida	0–700	22	0.053	356–2,000	0.003	5–10	10	32
C. microdon	1,000–1,300	31	0.032	237–1,000	0.004	2–4	7	14
C. microdon	1,000–1,300	34	0.032	43–392	0.003	2–4	11	27
C. microdon	1,000–1,300	36	0.031	442–1,000	0.004	2–4	9	33
C. microdon	1,000–1,300	40	0.028	150–806	0.001	2–7	19	38

SL, standard length; N, Number; Diam, diameter; Capi, capillary.

TABLE 4 Equations and parameters of the linear regressions between percentage area with fat tissue (FT) and standard length (SL) for *Cyclothone* species.

Specie	Equation	F	R^2	p-value	r	N
C. pygmaea	FT = 2.03 + 3.43 SL	28.46	0.803	0.001	0.896	9
C. pallida	FT = 11.02 + 2.39 SL	49.66	0.832	0.0001	0.910	13
C. livida	FT = 15.99 + 1.64 SL	15.99	0.762	0.01	0.873	7
C. microdon	FT = 10.19 + 2.30 SL	83.76	0.815	0.0001	0.902	21

F, F-statistic; R^2, coefficient of determination; r, Pearson of correlation; N, number of individuals.

the equation $ESR = (a * b * c)^{1/3}$, where *c* is the width of the semi-axis (*SwW/2*) (Strasberg, 1953). The aspect ratio (E) was calculated as the ratio of the height to the longitudinal semi-axis (c/*a*).

2.4 Body mass density

Body mass density (ρ) was determined *via* a density-bottle method (Greenlaw, 1977; Mikami et al., 2000) for the four species sampled during the *SUMMER* survey above 700 m depth (*C. braueri*, *C. pseudopallida*, *C. pygmaea*, and *C. pallida*) (n = 128; Table 1). The buoyancy of each individual fish was measured using a series of 1,000-ml beakers containing seawater–glycerol solutions of different densities (14 bottles from 1.025 to 1.090 g/cm^3 at 0.005 g/cm^3 steps). The density of each bottle was confirmed using a glass densimeter (standard at 20°C), and the experiment was carried out in a thermoregulated room to keep the solution in each bottle at 20° C. Gas was removed from the organisms with a sharp needle before measurements. The density contrast *g* was obtained by dividing ρ by the density of the surrounding seawater (ρ_w, the average of seawater densities in the depth stratum). Statistical analyses (ANOVA) were applied to identify significant differences in body mass density between species. The Tukey's Honest Significant Differences *Post Hoc* test (HSD) was used to assess statistical differences between pairs of groups from the analysis of variance that was previously applied.

The gas volume required for neutral buoyancy (V_G) was calculated following the equation. $V_G = W_W(\rho_w^{-1} - \rho_f^{-1})$. in Taylor (1951), where *Ww* is the wet weight and ρf is the body mass density for each individual. The Pearson correlation coefficient (r) was used to evaluate the linear correlation between body mass density and standard length.

The analyses of this study were developed in the programming language R (R Core Team, 2022). The sampling map was generated using the geographic information system QGIS (V.3.22.3) (QGIS Development Team, 2022).

3 Results

Five species of the *Cyclothone* genus were collected in the North Atlantic Ocean (*C. braueri*, *C. pseudopallida*, *C. pallida*, *C. livida*, and *C. microdon*), while only *C. pygmaea* and *C. braueri* were collected in the Mediterranean Sea. The most abundant species were *C. braueri*, *C. livida*, and *C. microdon*, accounting for >80% of total *Cyclothone*, while in terms of biomass, the major contributions were from *C. microdon*, *C. livida*, and *C. braueri*. Shallower species (*C. braueri* and *C. pseudopallida*) were found

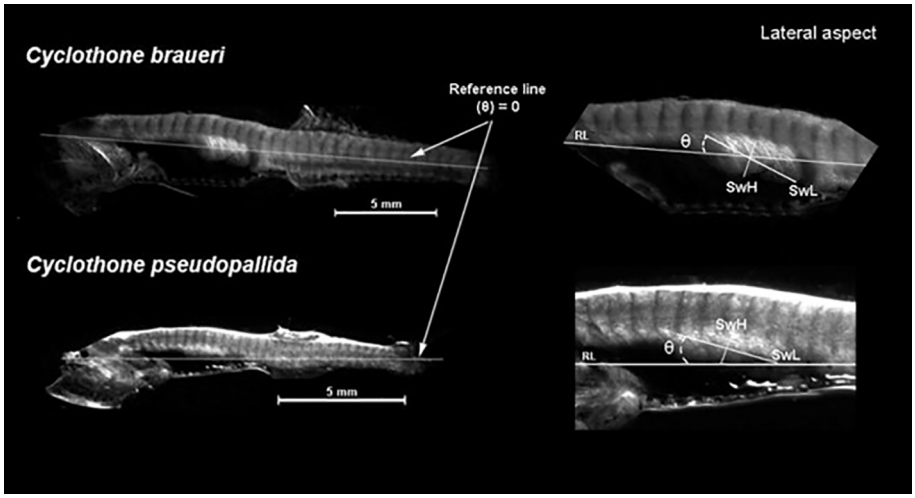

FIGURE 2
Cyclothone spp. swimbladder measurements performed with a microscope. SwL is swimbladder length; SwH is swimbladder height; SwW is swimbladder width; and θ is swimbladder angle. RL is the reference line.

between 200 and 600 m depths, while the deeper species (*C. pallida* and *C. microdon*) were mainly found below 800 m depths. *C. microdon* increased in abundance northward of 30°N, and *Cyclothone livida* was mainly sampled in the oceanic upwelling off Northwest Africa from 400 to 1,900 m depths. In terms of biomass, most of *C. braueri* biomass was observed between 200 and 600 m depths from 20 to 60°N. *Cyclothone pseudopallida* and *C. livida* showed a wider biomass vertical distribution (200–800 m depths and 450–1,900 m depths, respectively), but the latter was only found from 18° to 45°N. The biomass of *C. microdon* showed the widest spatial (18°–54°N) and vertical distributions (450–1,900 m depths).

Standard length ranges (Figures 3, 4) were narrower for *C. braueri*, *C. pseudopallida*, and *C. pygmaea* (range: 10–35 mm SL) than for the other species (range: 11–55 mm SL). No significant differences in length were found between the day and night samples. Most species showed a bimodal size distribution at every 200 m depth stratum. Shallower species were smaller than deeper species (Shallower, 200–400 m: 10–33 mm SL; 400–600 m: 10–33; 600–800 m: 9–23 mm SL; 800–1,000 m: 10–35 mm SL; Deeper, 200–600 m: 14–42 mm SL; 800–1,200 m: 11–51 mm; 1,200–2,000 m: 15–55 mm SL).

Histological examination of the swimbladder features was carried out for *C. braueri* (n = 80), *C. pseudopallida* (n = 14), *C. pallida* (n = 55), *C. pygmaea* (n = 18), *C. livida* (n = 8), and *C. microdon* (n = 19). The swimbladder of these species is located above the gonads and the gastro-intestinal system (GI) and below the spinal cord (SC) and notochord (NT). It begins at the level of the gastro-intestinal system and ends around the origin of the pelvic fin (Figure 5). *C. braueri* and *C. pseudopallida* are shallower, semi-transparent species for which the swimbladder was measured with a microscope, while darker species comprised the second group that were analyzed exclusively through histology (no information on swimbladder size). In general, all species showed gas gland and *rete mirabile* (as physoclistous fishes; Figure 6). However, the deeper species with larger sizes presented reduced gas gland and *rete mirabile* (0.032 and 0.004 mm^2, respectively), i.e., reduced total and cell area, a lower number of capillaries, and smaller capillaries than other deep species of smaller size (*C. pallida*; 0.053 and 0.003 mm^2) (see Figures 7 and Table 3), indicating a deterioration in swimbladder functionality with age and depth.

The body mass density (ρ) of the four *Cyclothone* spp. (*C. braueri*, *C. pseudopallida*, *C. pygmaea*, and *C. pallida*) sampled from the surface to 700 m depth in the Mediterranean Sea ranged from 1.055 to 1.072 g cm^{-3} (1.061 ± 0.004 g cm^{-3}; g = 1.026–1.045). Significant differences were observed among the three species ($F_{2,124}$ = 14.19, p<0.001; *C. braueri*: 1.061 ± 0.004; *C. pallida*: 1.057 ± 0.003; and *C. pseudopallida*: 1.062 ± 0.004 g cm^{-3};

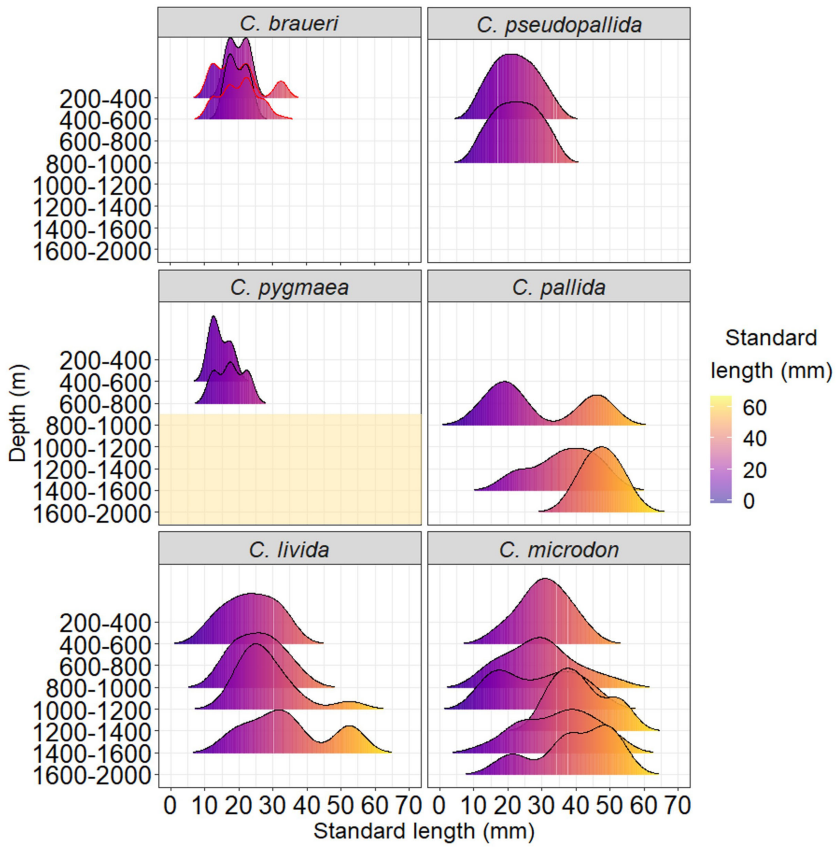

FIGURE 3
Length distribution of *Cyclothone braueri*, *C. pseudopallida*, *C. pallida*, *C. livida*, and *C. microdon* by size classes and depths collected with the MOCNESS-1 net (200 µm of mesh size) in the northeast Atlantic during the Bathypelagic cruise. *C. braueri* with a red contour and *C. pygmaea* data were obtained in the western Mediterranean during the SUMMER cruise. Shaded areas in *C. pygmaea* indicate not sampled depths.

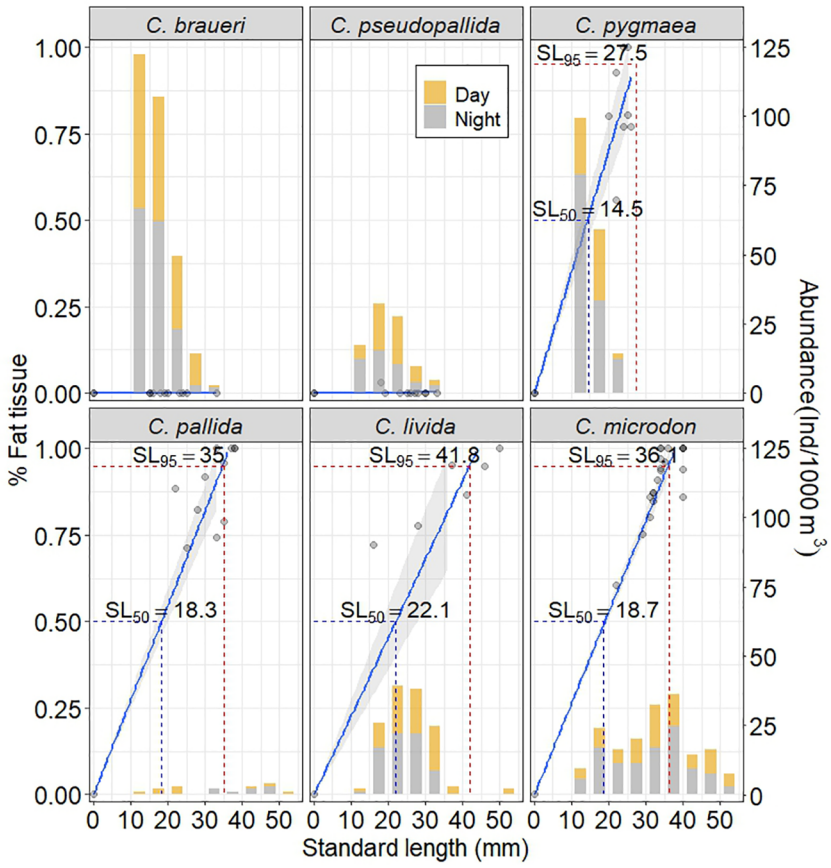

FIGURE 4
Linear regression model fit predicting the percentage of fat tissue in *Cyclothone* spp. swimbladders from standard length (mm) assuming zero percentage at the origin (left vertical axis) and size frequency distribution (right vertical axis). SL_{50}, half-filled swimbladder of fat tissue (50%); SL_{95}, lipid-full swimbladder (95%).

Table 7 and Figure 8A), where the Tukey test showed significant differences between *C. braueri* and *C. pallida* ($p<0.001$). There was a slight negative correlation between *Cyclothone* body mass density and standard length ($r = -0.39$; $N = 127$; $p<0.001$) and depth ($r = -0.39$; $N = 127$; $p<0.001$). Although we found a rather low coefficient of determination (R^2), the correlation between *Cyclothone* body-mass density and standard length was significant ($r^2 = 0.15$; $p<0.001$), and significant differences in body-mass density could be established for *C. pseudopallida* ($p<0.05$, Tables 5, 7 and Figure 8). The species of *Cyclothone* with lower mass density (*C. pseudopallida* and *C. pallida*) were sampled at 450 and 650 m depth, respectively, while species with high ρ values (*C. braueri* and *C. pygmaea*) were found between 350 and 550 m (Figure 8B).

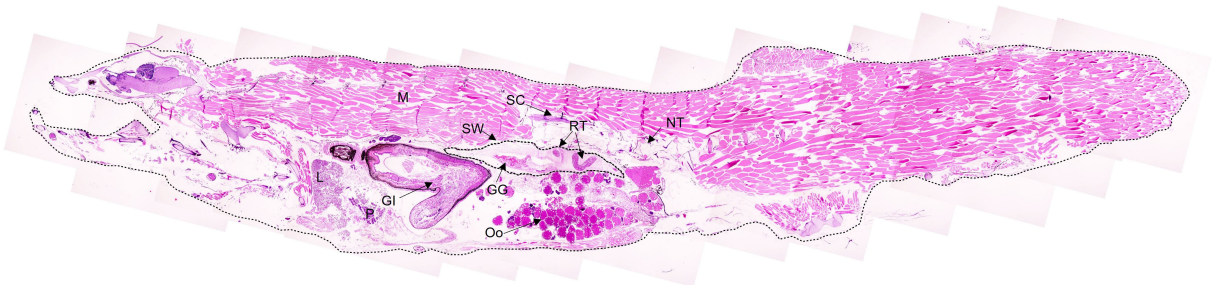

FIGURE 5
Histological image composition of a 20 mm *C. braueri* showing a longitudinal section of a specimen from head to midtail region. GG stands for Gas Gland, GI for Gastro-Intestinal, L for Liver, M for Muscle, NT for Notochord, P for Pancreas, Oo for Oocytes, RT for *rete mirabile*, SC for Spinal cord, and SW for Swimbladder.

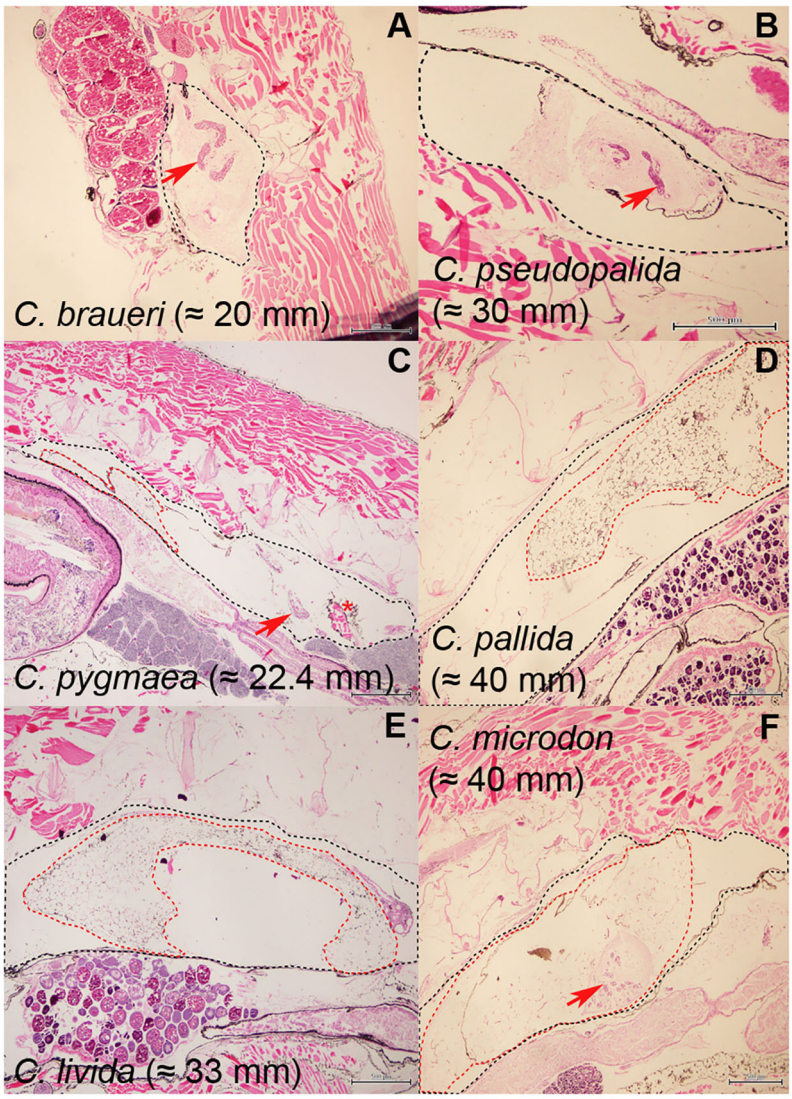

FIGURE 6
Histological sections of **(A)** *C. braueri* and **(B)** *C. pseudopallida* and for deeper species (**(C)** *C. pygmaea*, **(D)** *C. pallida*, **(E)** *C. livida*, and **(F)** *C. microdon*). The asterisk indicates the Gas gland, and the arrow the rete mirabile. The black contour delineates the swimbladder and the red contour the fat tissue.

3.1 *Cyclothone braueri*

C. braueri was the only species observed in both sampling areas (the northeast Atlantic and the Mediterranean Sea) and showed similar length distributions in both cases. *C. braueri* presented two modal size classes at 10–15 and 15–20 mm SL, although the larger size class was in the upper layer (200–400 m depth), with a bimodal size distribution (20 and 31 mm SL; Figures 3, 4). According to the vertical distribution, *C. braueri* was identified as an upper mesopelagic group (200–00 m) both in the Atlantic and the Mediterranean Sea (10–30 mm SL) and is characterized by its semitransparent color with light pigmentation. A total of 80 individuals were examined for histological analysis. This species did not present fat tissue (Figure 6), and the regression line was flat both in the Atlantic and the Mediterranean Seas (Figure 4). The abundance and biomass of *C. braueri* individuals with no fat tissue were high between 200 and 550 m depth in the North Atlantic Ocean (Figures 9A, B) and from 300 to 700 m depth in the Mediterranean Sea (Figure 9C).

A total of 215 individuals were used to measure the morphological features of the swimbladder (Figure 10). *C. braueri* showed a longer, more flattened, and less wide swimbladder than *C. pseudopallida* (Table 5). We observed significant relationships between swimbladder length, height, width, and standard length. Swimbladder angle and standard length were not significantly correlated. Negative allometric growth was inferred for swimbladder height with standard length, while swimbladder width showed positive allometric growth (Table 6). Swimbladder volume and equivalent radius (ESR) were also significantly correlated with standard length ($p<0.05$), with a negative allometric growth (Figure 11 and Table 6).

Body mass density (ρ) collected between 350 and 550 m in the Mediterranean Sea ranged from 1.052 to 1.072 g·cm^{-3} (1.061 ± 0.004 g cm^{-3}; Table 7 and Figure 11). The amount of gas required

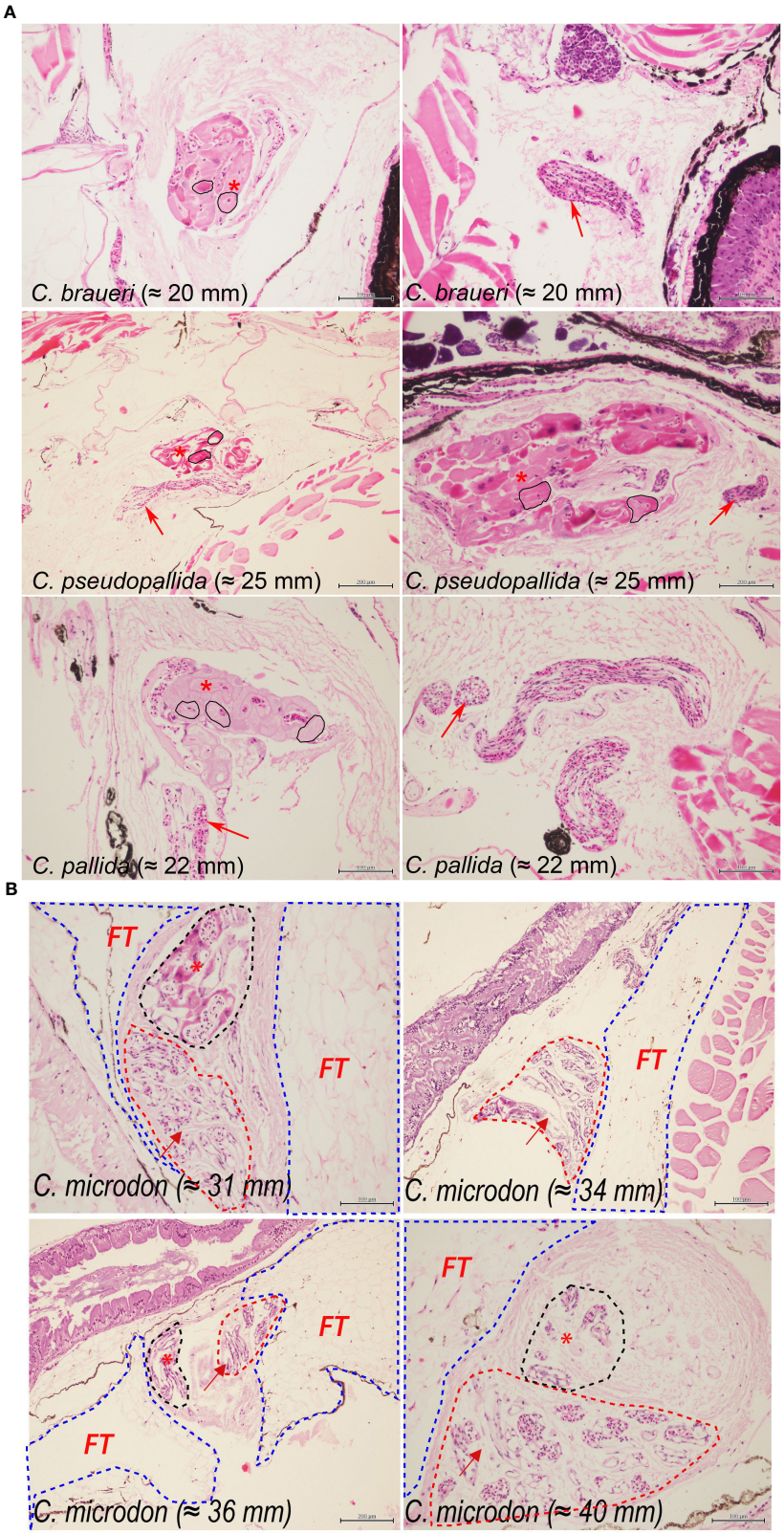

FIGURE 7
(A) Histological sections of *C. braueri* (20 *mm*), *C. pseudopallida* (25 and 19 mm), and *C. pallida* (19 *mm*). The asterisk indicates the Gas gland, and the arrow indicates the *rete mirabile*. The black contour delineates the area of gas gland. * *C. braueri* and *C. pallida* panels show different sections of the same individual. **(B)** Histological sections of *C. microdon* individuals. The asterisk indicates the Gas gland, and the arrow indicates the *rete mirabile*. The blue contour delineates the fat tissue, the red contour the rete mirabile, and the black contour the gas gland.

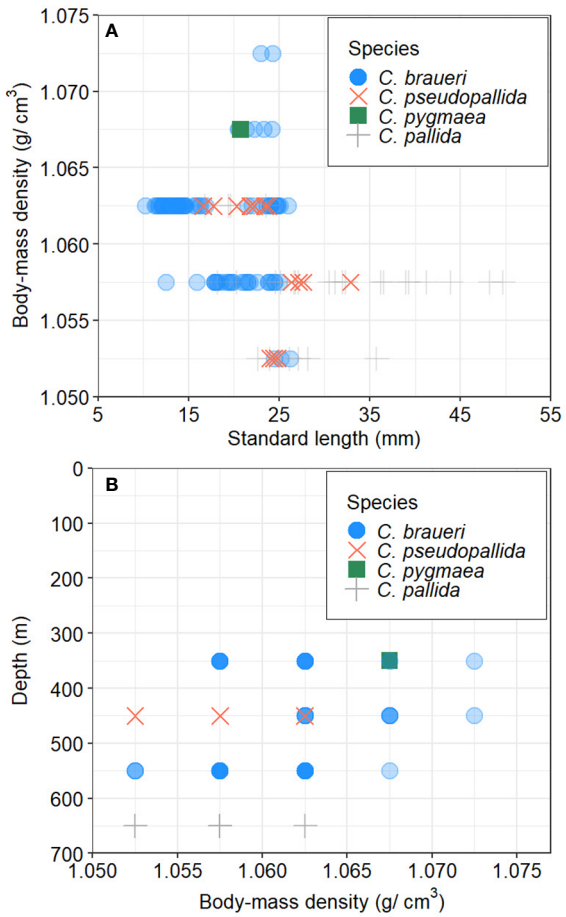

FIGURE 8
Relationship between body-mass density (ρ, g·cm^{-3}) and **(A)** standard length (mm), and **(B)** depth (m) by *Cyclothone* species.

for neutral buoyancy (V_G) varied with size and species (range 2%–4%). Both minimum and maximum values were found in *C. braueri* (10.3–26.2 mm SL).

3.2 *Cyclothone pseudopallida*

C. pseudopallida, distributed in the Northeast Atlantic Ocean, presented two modal size classes at 15–20 and 20–25 mm SL (Figures 3, 4 and Table 4). According to the vertical distribution, this species was identified as an upper mesopelagic group (200–600 m; 10–30 mm SL) and is characterized by its semitransparent color with light pigmentation. The size distribution did not show changes with depth. However, this species has a slightly deeper distribution than *C. braueri* (WMD: 677.1 and 547.1 m depth, respectively). A total of 14 individuals were examined for histological analysis. This species did not present fat tissue (Figure 7). The regression model between the percentage of area with fat tissue and standard length was not significant for this species (Figure 4 and Table 4). However, one individual showed a low percentage of fat tissue (3.17%; 18 mm SL). *C. pseudopallida* individuals with no fat tissue were abundant towards the south of the studied area (as biomass), while the maximum percentage of gas (%GAS) gradually decreased for deeper and northern species (Figures 9).

A total of 38 individuals were used to measure the morphological features of the swimbladder. Swimbladder length (SwL) ranged from 0.5 to 4.6 mm, with slightly higher mean lengths for *C. pseudopallida* than for *C. braueri*. Swimbladder height (SwH) ranged from 0.4 to 1 mm. No differences in swimbladder width (SwW) (0.5–2 mm) were observed between semi-transparent species. We observed significant relationships between swimbladder length, width, and standard length (Figure 10). Swimbladder angle and standard length were not significantly correlated. A negative allometric growth was inferred for swimbladder height with standard length, while swimbladder width was isometric (Table 6). Swimbladder volume and equivalent radius (ESR) were also significantly correlated with standard length ($p<0.05$), with a negative allometric growth (Figure 11 and Table 6).

Body mass density (ρ) collected between 450 and 700 m in the Mediterranean Sea ranged from 1.052 to 1.062 g·cm^{-3} (1.061 ± 0.004 g cm^{-3}; Table 7 and Figure 8). The amount of gas required for neutral buoyancy (V_G) varied with size and species (range 2%–4%). *C. pseudopallida* was between 2.8 and 3.25% (16.6–32.9 mm with 2.8%).

3.3 *Cyclothone pygmaea*

C. pygmaea was the only species distributed in the Mediterranean Sea, with the lowest modal size class at 10–15 mm SL (Figure 3). *C. pygmaea*, characterized by its brown color, was identified as a lower mesopelagic group (region below 600 m depth) in the Mediterranean Sea (600–700 m; 10–25 mm SL) with a highly multimodal size distribution at 600–800 m depth (12, 16, and 22 mm SL). A total of 18 individuals were examined for histological analysis. The swimbladders of *C. pygmaea* individuals (20–26 mm) had a high percentage of the area filled with fat tissue, reaching a half-filled swimbladder at 14.5 mm (the maximum standard length is 26 mm) (Figure 4). Individuals collected in the lower mesopelagic zone presented 78.5% fat tissue in the swimbladder (Figure 7). The maximum percentage of gas (%GAS) gradually decreased with depth in the Mediterranean Sea sampled from 0 to 700 m (Figure 9C), where the percentage of area with gas varied from 29% to 46% at the maximum.

Body mass density (ρ) collected between 350 and 550 m in the Mediterranean Sea ranged from 1.052 to 1.062 g·cm^{-3} (1.061 ± 0.004 g cm^{-3}; Table 7 and Figure 8). The amount of gas required for neutral buoyancy (V_G) was 3.6% for 20.77 mm SL.

3.4 *Cyclothone pallida*

C. pallida, distributed in the Northeast Atlantic Ocean, presented two modal size classes at 20–25 and 40–50 mm SL (Figures 3, 4). It was identified as a deeper meso- and bathypelagic group in the Atlantic (400–1,800 m; WMD: 1,150 m) and is characterized by its brown color. We found multimodal size classes in the lower mesopelagic layer (18 and 44 mm SL) and

10.3389/fmars.2023.1093982

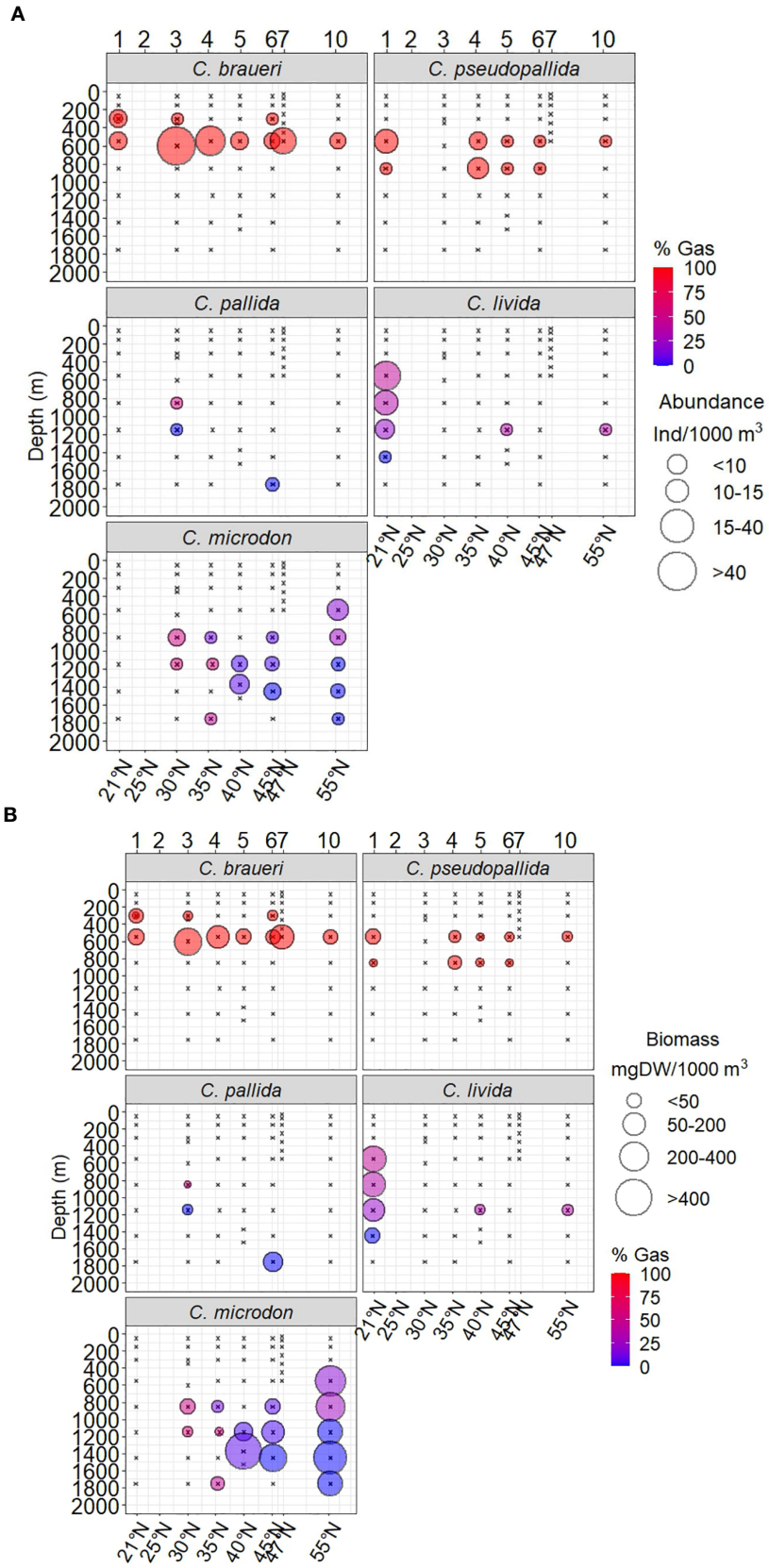

FIGURE 9 (Continued)

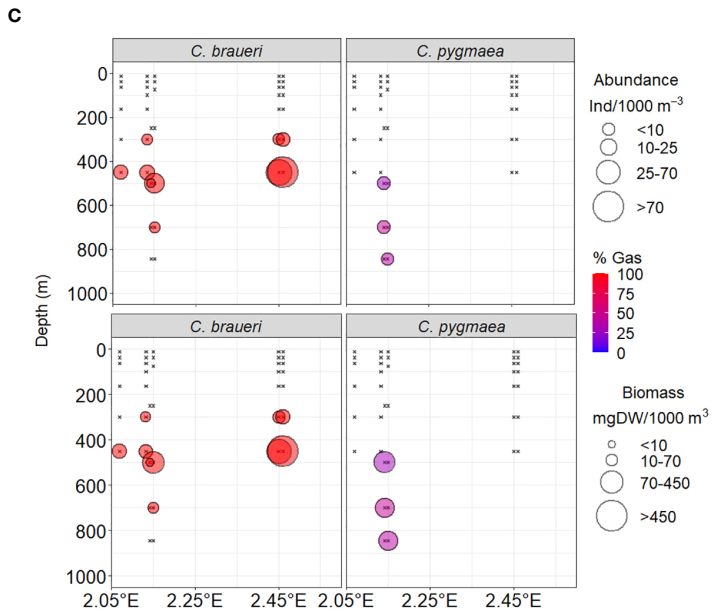

FIGURE 9 (Continued)
(A) Vertical distribution of fish abundance (dots size) and swimbladders maximum percentage of area with gas (color fill) for *C. braueri*, *C. pseudopallida*, *C. pallida*, *C. livida*, and *C. microdon* collected with the MOCNESS-1 net (200 µm of mesh size) in the northeast Atlantic during the Bathypelagic cruise. **(B)** Vertical distribution of fish biomass (dot size) and swimbladders maximum percentage of area with gas (color fill) for *C. braueri*, *C. pseudopallida*, *C. pallida*, *C. livida*, and *C. microdon* collected with the MOCNESS-1 net (200 µm of mesh size) during Bathypelagic cruise in the North Atlantic Ocean. **(C)**. Vertical distribution of fish abundance, biomass (dot size), and swimbladders maximum percentage area with gas (color fill) for *C. braueri and C. pygmaea* collected with the MOCNESS-1 net (200 µm of mesh size) during the IDEADOS cruise in the Western Mediterranean Sea.

between 1,400 and 1,600 m depth (22 and 40 mm SL). The SL–depth relationship showed a significant positive correlation (r = 0.58, $p<0.05$). A total of 55 individuals were examined for histological analysis. The regression model between the percentage of area with fat tissue and standard length showed that specimens that reached the bathypelagic layers exhibited 50% swimbladder fat content at 18.3 *mm* SL (which are within the 15th and 23rd quantiles of their standard-length distribution). Moreover, these individuals (20–50 mm SL) showed a higher variability in the content of fat tissue (FT: 89.4 ± 10.9%). An almost lipid-full swimbladder (SL_{95}) was reached at 35 mm SL (Figure 4). The cells of the gas gland in the small specimens were large, such as those of shallower species (*C. braueri* and *C. pseudopallida*, 20 *mm* SL) (see Table 3). The specimens showed a 17% increase in fat tissue size (from 28.5 to 40 mm SL; Figure 7). Individuals of *C. pallida* showed a latitudinal variation in the gas percentage between 28% and 55% at 800 m depth (Figure 9C).

Body mass density (ρ) collected between 450 and 700 m in the Mediterranean Sea ranged from 1.052 to 1.062 g·cm^{-3} (1.061 ± 0.004 g cm^{-3}; Table 7 and Figure 8). The amount of gas required for neutral buoyancy (V_G) for deeper species was 2.6%–3.1% of gas volume for individuals between 16.8 and 49.7 mm SL.

3.5 *Cyclothone livida*

C. livida, distributed in the Northeast Atlantic Ocean, presented two modal size classes at 20–25 and 25–30 mm SL (Figures 3, 4). It was identified as a deeper meso- and bathypelagic group in the Atlantic (400–1,800 m; WMD: 790.9 m) and is characterized by its brown color. This species showed a bimodal size class in the bathypelagic layer (25 and 52 mm SL at 1,000–1,200 m depth and 32 and 52 mm SL at 1,400–1,600 m depth; Figure 3). The SL–depth relationship showed a significant positive correlation (r = 0.424, $p<0.05$; $SL–Depth_{<1,000\ m}$ r = 0.34, $p<0.05$).

A total of eight individuals were examined for histological analysis. The regression model between the percentage of area with fat tissue and standard length showed that specimens that reached the bathypelagic layers exhibited 50% swimbladder fat content at 22.1 *mm* SL (which is within the 15th and 23rd quantiles of their standard-length distribution). The lipid-full swimbladder in *C. livida* was within the maximum values of SL, although the larger sizes were less abundant. An almost lipid-full swimbladder (SL_{95}) was reached at 41.8 mm SL (Figure 4). The specimens showed a 23% increase in fat tissue size (from 16 to 33 mm SL; Figure 7). A summary of all fat tissue measurements is included in Table 2. The abundance, biomass, and gas content of *C. livida* decreased with depth (35%–45% gas between 550–850 m depth and 35%–0% gas between 1,150 and 1,800 m depth) (Figures 9).

3.6 *Cyclothone microdon*

C. microdon, distributed in the Northeast Atlantic Ocean showed the largest modal size classes at 30–35 mm and 35–40

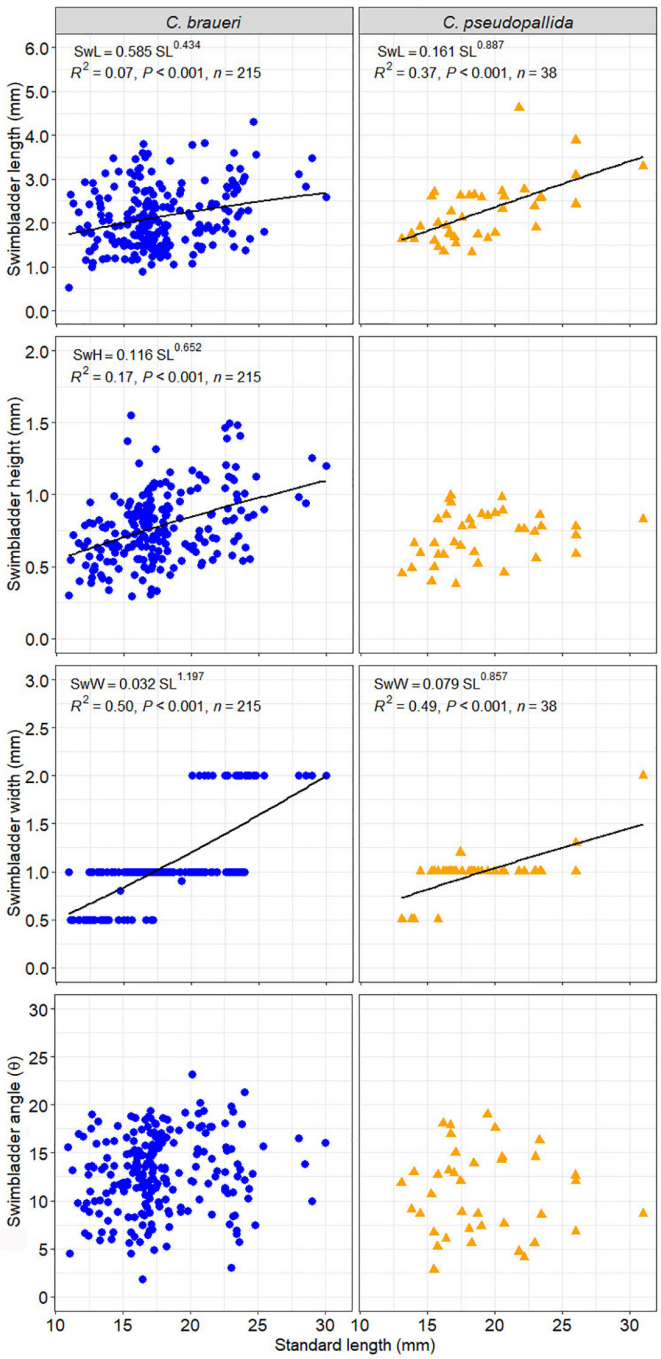

FIGURE 10
Relationship between standard length and swimbladder length (SwL), height (SwH), width (SwW), and angle (Swθ) for *C. braueri* (blue dots) and *C. pseudopallida* (yellow dots).

mm SL, and the lowest one at 15–20 mm (Figures 3, 4). As in the two deeper species mentioned above, this species had larger size classes below 800 m. It was identified as a deeper meso- and bathypelagic group (400–1,800 m; WMD: 1123.7 m) and is characterized by its brown color. We found multimodal size classes in the lower mesopelagic layer (18 and 30 mm SL) and between 1,200 and 1,400 m depth (38 and 52 mm SL; Figure 3). The SL–depth relationship showed a significant positive correlation (SL–$Depth_{>1,000\ m}$ r = 0.43, p<0.05).

A total of 19 individuals were examined for histological analysis. The regression model between the percentage of area with fat tissue and standard length showed that specimens that reached the bathypelagic layers exhibited 50% swimbladder fat content at 18.7 *mm* SL (which are within the 15th and 23rd quantiles of their standard-length distribution). These individuals (20–50 mm SL) showed higher variability in the content of fat tissue (FT: 89.3 ± 10.8%). An almost lipid-full swimbladder (SL_{95}) was reached at 36.1 mm SL. The SL_{95} was within the main size class model

10.3389/fmars.2023.1093982

TABLE 5 Measurements of the swimbladder of semi-transparent *Cyclothone* spp. examined in this study.

	Symbol	Unit	Range	Mean ± SD	Species
Standard length	*SL*	mm	10.92–30.00	17.68± 3.63	*C. braueri*
			13.08–31.00	19.06 ± 4.02	*C. pseudopallida*
Swimbladder Length	*SwL*	mm	0.53–4.31	2.13 ± 0.69	*C. braueri*
			1.34–4.63	2.25 ± 0.70	*C. pseudopallida*
Swimbladder Height	*SwH*	mm	0.30–1.55	0.78 ± 0.24	*C. braueri*
			0.38–0.99	0.71 ± 0.17	*C. pseudopallida*
Swimbladder Width	*SwW*	mm	0.5–2	1.04 ± 0.37	*C. braueri*
			0.5–2	0.99 ± 0.24	*C. pseudopallida*
Swimbladder angle	*Swθ*		1.84–23.13	12.82 ± 3.98	*C. braueri*
			2.80–19.01	10.81 ± 4.43	*C. pseudopallida*
Long lateral semi-axis	*a*	mm	0.26–2.15	1.06 ± 0.34	*C. braueri*
			0.67–2.31	1.13 ± 0.35	*C. pseudopallida*
Short lateral semi-axis	*b*	mm	0.15–0.77	0.38 ± 0.12	*C. braueri*
			0.19–0.49	0.35 ± 0.08	*C. pseudopallida*
Short dorsal semi-axis	*c*	mm	0.25–1.00	0.52 ± 0.19	*C. braueri*
			0.25–1.00	0.49 ± 0.12	*C. pseudopallida*
Equivalent radius (ESR)	$(a{\cdot}b{\cdot}c)^{1/3}$	mm	0.27–1.03	0.58 ± 0.14	*C. braueri*
			0.36–0.87	0.57 ± 0.11	*C. pseudopallida*
Aspect ratio	$E = c/a$		0.16–1.88	0.54 ± 0.26	*C. braueri*
			0.21–0.74	0.46 ± 0.12	*C. pseudopallida*

SD, standard deviation.

TABLE 6 Parameters of regressions of swimbladder measurements (Sw_i, mm) and standard length (SL, mm) for semi-transparent *Cyclothone* species in Atlantic waters $Sw_i = p * SL^q$ CL (confidence interval).

Species	p	q	Inferior 95% CL of q	Superior 95% CL of q	R^2	Growth model
	Swimbladder Length–Standard Length relationship					
C. braueri	0.59	0.43	0.22	0.65	0.07	a^-
C. pseudopallida	0.16	0.89	0.51	1.27	0.38	i
	Swimbladder Height–Standard Length relationship					
C. braueri	0.12	0.65	0.45	0.84	0.17	a^-
C. pseudopallida	0.20	0.42	0.01	0.83	0.11	a^-
	Swimbladder Width–Standard Length relationship					
C. braueri	0.03	1.19	1.03	1.35	0.49	a^+
C. pseudopallida	0.08	0.85	0.53	1.18	0.44	i
	Swimbladder angle–Standard Length relationship					
C. braueri	6.63	0.21	−0.04	0.45	0.01	a^-
C. pseudopallida	12.2	−0.07	−0.85	0.71	0.01	a^-
	Swimbladder volume–Standard Length relationship					
C. braueri	0.001	2.28	1.91	2.65	0.42	a^-

(Continued)

TABLE 6 Continued

Species	p	q	Inferior 95% CL of q	Superior 95% CL of q	R^2	Growth model
C. pseudopallida	0.001	2.16	1.45	2.87	0.52	a^-
	Equivalent radius–Standard Length relationship					
C. braueri	0.06	0.76	0.64	0.88	0.41	a^-
C. pseudopallida	0.06	0.72	0.48	0.95	0.52	a^-
	Aspect ratio–Standard Length relationship					
C. braueri	0.05	0.76	0.47	1.05	0.10	i
C. pseudopallida	0.48	−0.03	−0.49	0.43	0.0004	a^-

p, intercept of the regression models and q, the slope. Growth model: negative allometric (a^-), isometric growth (i), positive allometric growth (a^+).

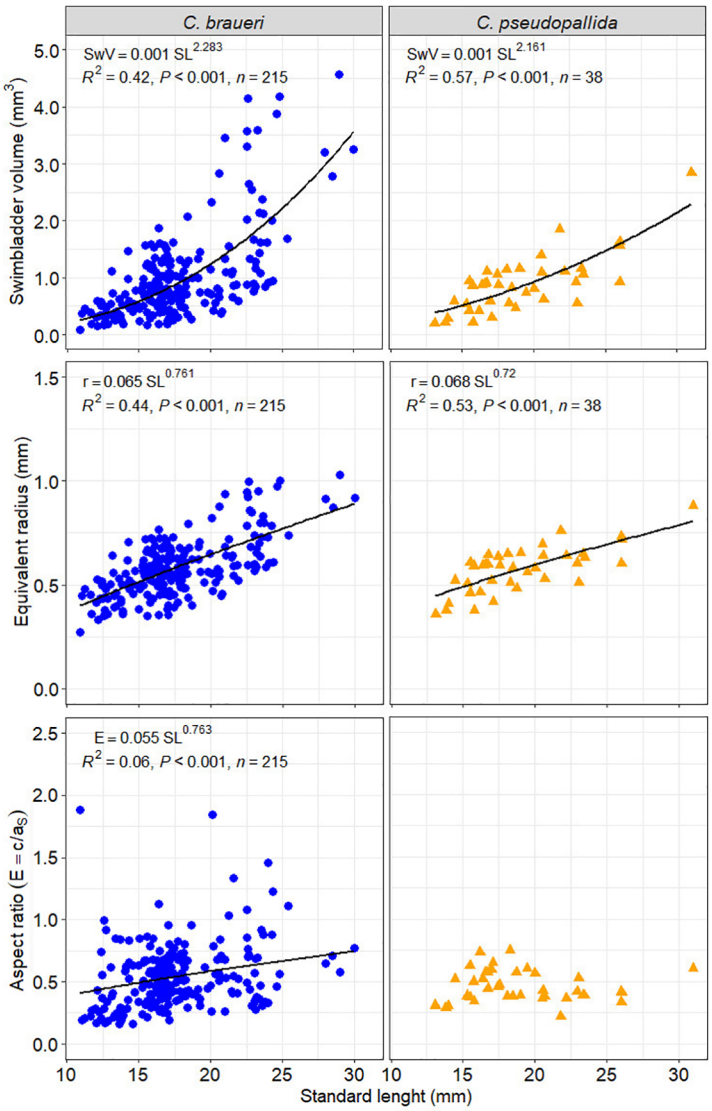

FIGURE 11
Relationship between standard length (SL, mm) and swimbladder volume (SwV), equivalent radius (r), and aspect ratio ($E = c/a$), where a is the longitudinal semi-axis and c the width semi-axis for *C. braueri* (blue dots) and *C. pseudopallida* (yellow dots).

TABLE 7 Summary of the body-mass density experiment results obtained for species sampled in Mediterranean waters down to 700 m depth.

Species/biological group	Standard length (mm)	Wet weight (g)	Body mass density (ρ, g·cm^{-3})	Density contrast (g)	N
Cyclothone braueri	10.26–26.25	2.89–68.02	1.052–1.072	1.020–1.040	83
Cyclothone pseudopallida	16.58–32.89	14.34–57	1.052–1.062	1.023–1.033	15
Cyclothone pygmaea	20.77	27.93	1.067	1.036	1
Cyclothone pallida	16.83–49.67	16.11–273	1.052–1.062	1.022–1.031	29
Mean ± SD	**21.84 ± 7.55**	**42.08 ± 43.72**	**1.060 ± 0.004**	**1.029 ± 0.004**	

SD, standard deviation.

(Figure 4). Moreover, the deep species with larger sizes presented reduced gas glands and *rete mirabiles* (0.032 and 0.004 mm^2, respectively), i.e., reduced total and cell area, a lower number of capillaries, and smaller capillaries than other deep species of smaller size (*C. pallida*; 0.053 and 0.003 mm^2) (see Figures 7 and Table 3), indicating a deterioration in swimbladder functionality with age and depth. According to abundance in vertical distribution and gas (Figure 9), we found three groups of *C. microdon* individuals: the first group was found between 30° and 35°N with high gas content (45%–58%); the second group, between 35° and 45°N, with 4%–12% gas; and the third group of individuals, distributed in the northern stations (55°N), with 17%–25% gas.

4 Discussion

This study provides basic biological parameters (length frequency distribution, swimbladder location within the body, fat tissue content, morphology, and morphometry) and acoustic properties (body mass density, density contrast, and gas volume required for neutral buoyancy) of bristlemouth species analyzed in the North Atlantic Ocean and Mediterranean Sea that are needed to improve the accuracy of backscattering models. Species diversity was different between the Atlantic (*C. braueri*, *C. pseudopallida*, *C. pallida*, *C. livida*, *and C. microdon)* and the Mediterranean (*C. braueri* and *C. pygmaea*) as previously reported in the literature (Goodyear et al., 1972; Badcock and Merrett, 1976; Badcock, 1982; Roe and Badcock, 1984; Olivar et al., 2012; Sarmiento-Lezcano et al., 2022). However, the only coincident species (*C. braueri*) had similar length and depth distributions in both areas. Our results as well as previous research showed that *Cyclothone* spp. can be grouped according to their distribution in the water column. Shallower species such as *C. braueri* and *C. pseudopallida* were found in the upper mesopelagic layer (Sarmiento-Lezcano et al., 2022), *C. pygmaea* in the lower mesopelagic layer (Goodyear et al., 1972), and *C. pallida*, *C. livida*, and *C. microdon* were observed in the meso- and bathypelagic layers (Badcock and Merrett, 1976; Badcock and Merrett, 1977; Marshall, 1979; Miya and Nemoto, 1986; Sarmiento-Lezcano et al., 2022). The *Cyclothone* species occupying the shallower layers tend to be more "transparent," while those found in deeper layers are "darkly colored" (Badcock, 1984). *Cyclothone* species are non-migrant organisms (Badcock and Merrett, 1976; Olivar et al., 2017; Sarmiento-Lezcano et al., 2022), widely distributed in the water column (from the mesopelagic to the bathypelagic zone), whose vertical distribution could be conditioned by water temperature, oxygen (Sarmiento-Lezcano et al., 2022), feeding type (Bernal et al., 2015; Thompson and Kenchington, 2017), and size of individuals (Agersted et al., 2021).

The size range of *Cyclothone* captured in the North Atlantic Ocean and Mediterranean Sea was like previous observations in the Atlantic Ocean (Equatorial and Tropical Atlantic, Olivar et al., 2017; Eastern of the Mid-Atlantic Ocean, Agersted et al., 2021). Badcock and Merrett (1976) showed a positive correlation between size and depth for *C. braueri*, *C. pseudopallida*, and *C. microdon*. In our study, we observed a similar correlation in *C. pallida*, *C. livida*, and *C. microdon* as larger individuals were found in the deeper layer (bathypelagic zone). Shorter species displayed a shallower location in the water column, close to the productive epipelagic layer. Deeper species appeared more adapted to minimizing energy expenses by limiting consumption rates and energy intake (Maynard, 1982). Species such as *Cyclothone pallida*, *C. livida*, and *C. microdon* showed a bimodal size distribution mainly in the bathypelagic zone, while *C. pygmaea* showed a multimodal size distribution between 600 and 800 m depth. Therefore, although deeper species are prone to be larger, less abundant modes of shorter species often cohabit at the same depths.

The swimbladder of shallower species was measured directly thanks to their semi-transparency. Measurements of swimbladder length, tilt angle, aspect ratio, and volume were lower in *Cyclothone* spp. than in other larger mesopelagic species previously examined (Kloser et al., 2002; Yasuma et al., 2003; Yasuma et al., 2006; Yasuma et al., 2010; Scoulding et al., 2015; Sobradillo et al., 2019; Escobar-Flores et al., 2020). Although the studied *C. pseudopallida* were larger than *C. braueri* (19.06 ± 4.02; 17.68 ± 3.63 mm SL, respectively), the lengths of their swimbladders were similar (2.25 ± 0.70; 2.13 ± 0.69 mm, respectively). Both species showed a negative allometric growth of the swimbladder versus body length. That is, the body grows relatively faster than the swimbladder. *C. braueri*, on the other hand, showed relatively faster growth of the swimbladder. Yasuma et al. (2010) observed that the swimbladder of myctophids showed positive allometric growth after the onset of gas secretion into the swimbladder. However, regressive growth or atrophy of the swimbladder is also common among myctophids (e.g., *Diaphus theta* and *Symbolophorus californiensis*) and a few other mesopelagic fishes during later stages (Butler and Pearcy, 1972; Neighbors and Nafpaktitis, 1982; Yasuma et al., 2010). The

equivalent spherical radius (ESR) values calculated in this study from direct swimbladder measurements (*C. braueri*: 0.27–1.03 and *C. pseudopallida*: 0.36–0.87 mm) agreed with those modeled for *Cyclothone* spp. by Agersted et al. (2021) (0.25–1.16 mm) and with previous measurements for *C. braueri* (0.6 *mm*) in Peña et al. (2014).

Histology is a technique often employed to study the swimbladder and its different components, such as the gas gland and *rete mirabile*, in non-transparent species (Marshall, 1960; Denton, 1961; Kuhn et al., 1963; Horn, 1975; Neighbors, 1992). This study shows that shallower *Cyclothone* spp. (*C. braueri* and *C. pseudopallida*) have functional physoclistous swimbladders with well-developed gas glands and *rete mirabiles* and with numerous capillaries. However, deeper, and larger *Cyclothone* species (*C. pygmaea*, *C. pallida*, *C. livida*, and *C. microdon*) present a fat-invested swimbladder and a contraction in the gas gland and *rete mirabile*. On the other hand, the coexistence of two length modes at the same depth strata seen above implies that a small percentage of the organisms sampled in deeper waters could still have some gas in their swimbladder. Horn (1975) also observed a regression of the gas gland in stromateoid fishes. As these species are larger than *Cyclothone* spp., their gas gland area (0.6–8.7 mm^2) and *rete mirabile* (0.4–2 mm) are also proportionally longer and start regressing at larger sizes (40–130 mm SL). Macdonald (1975) found a correlation between *rete mirabile* length and depth in the case of non-regressed swimbladders and a reduction in the number of capillaries in deep species due to degeneration of the swimbladder, as also found for *Cyclothone* spp. in our study (see Table 3).

The accumulation of lipids in deeper species provides stable buoyancy and a long-term energy reserve (Butler and Pearcy, 1972). Horn (1975) found that the swimbladder degenerates with increasing fish size, first becoming non-functional and ultimately existing only as a small remnant or disappearing completely. Similarly, Neighbors (1992) reported the atrophy and degradation of cellular components in the swimbladder with age, as observed in this study. It is difficult to establish the exact length at which the swimbladder becomes non-functional for deeper *Cyclothone* species, and we have no evidence of the gas content, but the high fat content and the indications of swimbladder degradation found in this study suggest that a high percentage of those individuals have no gas in their swimbladders. Swimbladder regression is a gradual process that makes it difficult to determine the exact length at which functionality is lost and the swimbladder stops to secrete or reabsorb gas. However, the large biomass of these species in the lower mesopelagic and bathypelagic zones, especially at northern latitudes (Sarmiento-Lezcano et al., 2022), and the low-scattering layers recorded acoustically (Peña, 2019), suggest that no gas is present in their swimbladders. Davison (2011) allocated small and large fish species to three groups based on the presence of gas in the swimbladders. The author observed that fish in group I showed increasing gas volume with increasing size, while fish in group II exhibited a decrease in the percentage of gas in the swimbladder with age, filling it with lipids. Species in group III never have inflated swimbladders. Davison (op. cit.) also observed the presence of gas in specimens of shallower species in the upper mesopelagic layer (*C. pseudopallida*, range: 18–43 mm, and *C. signata*, range: 15–35 mm), but not for deeper species in the bathypelagic layer (*C. acclinidens* and *C. pallida*). Marshall (1960) reported the presence of fat tissue in all *Cyclothone* spp. Examined, with the swimbladder fully adipose in adults of *C. braueri* (larger than 35 mm) and *C. livida* (larger than 37 mm). We did not find this organ regression in *C. braueri*, probably because our largest specimens were smaller than 31 mm. By contrast, we found swimbladder regression in *C. pygmaea*, *C. pallida*, *C. livida*, and *C. microdon* starting at 16.5, 17.7, 16, and 21.4 mm SL, respectively. Our predictive model determined that 95% of the *C. pygmaea*, *C. pallida*, *C. livida*, and *C. microdon* swimbladders were occupied by fat tissue at 29.2, 35.8, 40.7, and 36 mm SL, respectively (see Figure 4). We found fat tissue content in the swimbladder was closely related to fish size and depth location in this deeper species (the larger and deeper, the more fat content), in contrast with the high gas content in the upper mesopelagic zone for *C. braueri* and *C. pseudopallida*. Moreover, semi-transparent species showed relatively faster growth in body length than swimbladder volume and equivalent spherical radius. On the other hand, body-mass density and gas required for neutral buoyancy were higher in *C. braueri* and *C. pygmaea* collected between 350 and 550 m than in *C. pallida* and *C. pseudopallida* sampled in the 450–700 m layer.

Meso- and bathypelagic fish swimbladder morphology can differ among species as intra- and interspecific variability is common (Marshall, 1951; Marshall, 1960). A functional physoclistous swimbladder in meso- and bathypelagic species is composed of a well-developed gas gland and a *rete mirabile* with numerous capillaries (Marshall, 1960; Denton, 1961; Kuhn et al., 1963; Horn, 1975; Neighbors, 1992). However, in some cases the swimbladder regresses and replaces its gas with fat tissue as the organism grows (Marshall, 1951; Marshall, 1960). Thus, the swimbladder volume occupied by gas decreases, and their walls thicken (Kleckner and Gibbs, 1972). Some mesopelagic fishes of the Myctophidae family also accumulate fat tissue in their swimbladders, although, in contrast to *Cyclothone* spp., adults of myctophid species with fat-invested swimbladders (*S. leucopsarus* and *D. theta*) can perform extensive vertical migrations without the need to regulate the swimbladder to the surrounding pressure (Taylor, 1968).

Density and sound speed contrast between the fish body and the surrounding seawater are also important parameters for acoustic scattering models that vary with species, morphology, and vertical distribution (Agersted et al., 2021). The proportion and composition of lipids in mesopelagic species vary with area or season as well as within species (Butler and Pearcy, 1972; Kayama and Nevenzel, 1974). *Cyclothone* density contrast values obtained in this study (1.02 to 1.04) were within previous reported ranges (0.98 to 1.07) for mesopelagic (*Stenobrachius leucopsarus*, *S. nannochir*, *Lampanycrus rirteri*, *L. regalis*, *D. theta*, *Tarletonbeania crenularis*, *Protomyctophum thompsoni*, *P. crockery;* Butler and Pearcy, 1972) and epipelagic fishes (*G. morhua*; Chu et al., 2003). Although there was some indication of density contrast variation with depth, the limited depth strata evaluated in this study (<700 m depth)

precluded us from establishing a clear relationship. However, it has been reported that Gonostomatidae fish species contain 3.1%–30% of lipids in relation to dry wet in the mesopelagic zone and 44% in the bathypelagic zone (Nevenzel and Menon, 1980). Body mass density differences between mesopelagic and bathypelagic *Cyclothone* species were also reported in previous studies (Childress and Nygaard, 1973; Kayama and Ikeda, 1975; Nevenzel and Menon, 1980; Bailey and Robison, 1986; Neighbors, 1988; Stickney and Torres, 1989; Childress et al., 1990; Davison, 2011), with shallower *Cyclothone* species (mesopelagic *C. pseudopallida* and *C. signata)* individuals showing a range of 1.048–1.078 g/ml) and the *Cyclothone* with regressed swimbladder (meso- and bathypelagic *C. acclinidens* and *C. pallida* individuals showing a range of 1.038–1.078 g/ml) (Davison, 2011; Agersted et al., 2021).

The gas required for neutral buoyancy (VG) in this study (0%–4%) was within the range (0%–5%) reported for mesopelagic species with different standard length and body density in Davison (2011), including some *Cyclothone* species such as *C. pseudopallida* VG: 2.1%–3.1%, ρ: 1.0500–1.0600; SL: 18–43 mm), *C. signata* (VG: 1.9%–4.7%, ρ: 1.0475–1.0775; SL: 15–35 mm), *C. atraria* (VG: 1.2%–2.9%, ρ: 1.0400–1.0575; SL: 21–47 mm), *C. acclinidens* (VG: 1.0%–4.7%, ρ: 1.0375–1.0775; SL: 25–61 mm), and *C. pallida* (VG: 1.2%–2.9%, ρ: 1.0400–1.0575; SL: 30–68 mm). A slight decrease in VG with depth was observed for organisms collected between 350 and 550 m and those sampled between 450 and 700 m.

Cyclothone spp. are known to account for much of the echo of the very dense scattering layer detected at 400–700 m depth at 38 kHz (Peña et al., 2014; Ariza et al., 2016) and could be responsible for deeper layers detected in the bathypelagic zone (Peña et al., 2021). To further pursue the acoustic study of these species, we need to employ accurate scattering models. The swimbladder gas content determines whether a gas-bearing or fluid-like model needs to be employed (Peña et al., 2023a, Peña et al., 2023b). This study contributes to a better understanding of the swimbladder regression process in *Cyctlothone* spp. and the areas of the northeast Atlantic Ocean and the Western Mediterranean Sea where each acoustic typology could be more expected. However, it also points out the need for the development of intermediate models that consider a partially regressed swimbladder that is filled with both lipids and gas. Further knowledge of the point at which gas is no longer needed (when lipids provide enough buoyancy) is also required.

5 Conclusion

In summary, swimbladder histological analysis revealed a physoclistous swimbladder structure in the six *Cyclothone* spp. analyzed. For upper mesopelagic species (*C. braueri* and *C. pseudopallida*), the non-regressed swimbladder remained throughout development. However, for the species in the lower mesopelagic and bathypelagic zones (*C. pygmaea*, *C. pallida*, *C. livida*, and *C. microdon*), the presence of fat tissue varied within species and sizes. A regression model estimated that for this last group of species, the swimbladder of *Cyclothone* larger than 36–41 mm SL would be completely invested in fat tissue. Thus, while all *Cyclothone* species possess a swimbladder, only small fish in early stages and semi-transparent species inhabiting the upper mesopelagic zone can be expected to contain gas. These species should be acoustically modeled as gas-bearing organisms. Species in the lower mesopelagic zone have some degree of swimbladder regression but could contain some gas. As the swimbladder area with no fat tissue showed irregular shapes, acoustic models representing prolate spheroids are probably not accurate for these organisms. On the other hand, around 90% of the abundance in the bathypelagic zone (mostly of *C. microdon*) is expected to have a gas-depleted swimbladder (particularly in northern latitudes), thus behaving acoustically as a fluid-like species. All the information gathered in this study can be used to improve the acoustic backscattering modeling of *Cyclothone* spp. and thus better infer knowledge from recorded echograms.

Data availability statement

Publicly available datasets were analyzed in this study. This data can be found here: Olivar et al. (2022) https://doi.org/10.1594/PANGAEA.947631 and Sarmiento-Lezcano et al. (2023) https://doi.org/10.1594/PANGAEA.95494.

Ethics statement

The animal study was reviewed and approved by the Spanish Ministry of Science and Technology proyect (Bathypelagic, CTM2016-78853-R).

Author contributions

AS-L contributed to the species identification, net data collection and processing and carried out the swimbladder measurement and the density experiment. MO contributed to the species identification, data analyses, supervision, and acted as a cruise leader in the SUMMER cruise. MJC performed and examined the histological analysis of the species. MC participated in the density experiment. SH-L designed and promoted the Bathypelagic project and acted as cruise leader in the Bathypelagic cruise. AC designed and controlled the MESOPELAGOS net during both cruises. MP designed and supervised this study and contributed to data curation, data processing, and editing of the manuscript. All authors contributed to article writing and approved the submitted version.

Funding

This research was funded by projects Bathypelagic (CTM2016-78853-R), Ideados (CTM2007-65844-C02-01-02-03), and Desafío (PID2020-118118RB-I00) from the Spanish Ministry of Science and Technology, "Sustainable Management of Mesopelagic Resources" (SUMMER, 817806) from European Union Horizon 2020 Research and Innovation Programme, and

the "South and Tropical Atlantic Climate-Based Marine Ecosystem Prediction for Sustainable Management" (TRIATLAS, 817578) from European Commission. AS-L was supported by a postgraduate grant (BES-2017-082540) from the Spanish Ministry of Science and Innovation.

Acknowledgments

We would like to thank the captain and crew of the *R/V Sarmiento de Gamboa* for their support and hard work during the cruise. We also wish to acknowledge the UTM technical support on board. MPO acknowledges the institutional support of the AEI 'Severo Ochoa Centre of Excellence' accreditation (CEX2019-000928-S).

Conflict of interest

The authors declare that the research was conducted in the absence of any commercial or financial relationships that could be construed as a potential conflict of interest.

Publisher's note

References

Agersted, M. D., Khodabandeloo, B., Klevjer, T. A., García-Seoane, E., Strand, E., Underwood, M. J., et al. (2021). Mass estimates of individual gas-bearing mesopelagic fish from *in situ* wideband acoustic measurements ground-truthed by biological net sampling. *ICES Mar. Sci.* 78 (10), 3658–3673. doi: 10.1093/icesjms/fsab207

Ahlstrom, E. H., Richards, W. J., and Weitzman, S. H. (1984). "Families gonostomatidae, sternoptychidae, and associated stomiiform groups: Development and relationships," in *Ontogeny and systematics of fishes*. Eds. H. G. Moser, W. J. Richards, D. M. Cohen, M. P. Fahay, A.W.K. Jr. and S. L. Richardson (Spec. Publ), 184–198.

Ariza, A., Landeira, J. M., Escánez, A., Wienerroither, R., Aguilar de Soto, N., Røstad, A., et al. (2016). Vertical distribution, composition and migratory patterns of acoustic scattering layers in the canary islands. *J. Mar. Syst.* 157, 82–91. doi: 10.1016/j.jmarsys.2016.01.004

Badcock, J. (1970). The vertical distribution of mesopelagic fishes collected on the SOND cruise. J. *Mar. Biol. Ass. UK.* 50, 1001–1044. doi: 10.1017/S0025315400005920

Badcock, J. (1982). A new species of the deep-sea fish genus cyclothone goode & bean (Stomiatoidei, gonostomatidae) from the tropical Atlantic. *J. Fish Biol.* 20, 197–211. doi: 10.1111/j.1095-8649.1982.tb03920.x

Badcock, J. (1984). "Gonostomatidae," in *Fishes of the north-Eastern Atlantic and the Mediterranean*. Eds. P. J. P. Whitehead, M. L. Bauchot, J. C. Hureau, J. Nielsen and X. X. X. E. Tortonese (Paris: UNESCO), 284–301.

Badcock, J., and Merrett, N. R. (1976). Midwater fishes in the eastern north Atlantic–i. vertical distribution and associated biology in 30° n, 23° W, with developmental notes on certain myctophids. *Prog. Oceanogr.* 7, 3–58. doi: 10.1016/0079-6611(76)90003-3

Badcock, J., and Merrett, N. R. (1977). "On the distribution of midwater fishes in the eastern north Atlantic," in *Oceanic sound scattering prediction*. Eds. N. R. Andersen and B. J. Zahuranec (New York: Plenum Press), 249–282.

Bailey, T. G., and Robison, B. H. (1986). Food availability as a selective factor on the chemical compositions of midwater fishes in the eastern North Pacific. *Mar. Biol.* 91, 131–141. doi: 10.1007/BF00397578

Bernal, A., Olivar, M. P., Maynou, F., and de Puelles, M. L. F. (2015). Diet and feeding strategies of mesopelagic fishes in the western Mediterranean. *Prog. Oceanogr.* 135, 1–17. doi: 10.1016/j.pocean.2015.03.005

Butler, J. L., and Pearcy, W. G. (1972). Swimbladder morphology and specific gravity of myctophids off Oregon. *J. Fish. Res.* 29, 1145–1150. doi: 10.1139/f72-170

Capen, R. L. (1967). Swimbladder morphology of some mesopelagic fishes in relation to sound scattering. *Res. Rep. U. S. Navy Electron. Lab.* 1447, 1–31.

Castellón, A., and Olivar, M. P. (2023). VERDA: A multisampler tool for mesopelagic nets. *J. Mar. Sci. Eng.* 11 (1), 72. doi: 10.3390/jmse11010072

Childress, J. J., and Nygaard, M. H. (1973). The chemical composition of midwater fishes as a function of depth of occurrence off southern California. *Deep Sea Res. Oceanographic Abstracts* 20 (12), 1093–1109. doi: 10.1016/0011-7471(73)90023-5

Childress, J. J., Price, M. H., Favuzzi, J., and Cowles, D. (1990). Chemical composition of midwater fishes as a function of depth of occurrence off the Hawaiian islands: food availability as a selective factor? *Mar. Biol.* 105, 235–246. doi: 10.1007/BF01344292

Chu, D., Wiebe, P. H., Copley, N. J., Lawson, L. G., and Puvanendran, V. (2003). Material properties of north Atlantic cod eggs and early-stage larvae and their influence on acoustic scattering. *ICES Mar. Sci.* 60, 508–515. doi: 10.1016/S1054-3139(03)00047-X

Davison, P. (2011). The specific gravity of mesopelagic fish from the northeastern pacific ocean and its implications for acoustic backscatter. *ICES J. Mar. Sci.* 68, 2064–2074. doi: 10.1093/icesjms/fsr140

Davison, P. C., Koslow, J. A., and Kloser, R. J. (2015). Acoustic biomass estimation of mesopelagic fish: Backscattering from individuals, populations, and communities. *ICES J. Mar. Sci.* 72, 1413–1424. doi: 10.1093/icesjms/fsv023

Denton, E. J. (1961). "The buoyancy of fish and cephalopods," in *Progress in biophysics and biophysical chemistry*. Eds. J. A. V. Butler, B. Katz and R. E. Zirkle (London, New York, Paris: Pergamon Press, Oxford), 178–234.

Escobar-Flores, P. C., O'Driscoll, R. L., and Montgomery, J. C. (2018). Spatial and temporal distribution patterns of acoustic backscatter in the New Zealand sector of the Southern Ocean. *Mar. Ecol. Prog. Ser.* 592, 19–35. doi: 10.3354/meps12489

Escobar-Flores, P. C., O'Driscoll, R. L., Montgomery, J. C., Ladroit, Y., and Jendersie, S. (2020). Estimates of density of mesopelagic fish in the Southern Ocean derived from bulk acoustic data collected by ships of opportunity. *Polar Biol.* 43, 43–61. doi: 10.1007/s00300-019-02611-3

FAO (1997). "Lanternfishes: A potential fishery in the northern Arabian Sea," in *Review of the state of world fishery resources: Marine fisheries. FAO fisheries circular no. 920* (Rome: FAO), 173.

FAO (2001). *Trilateral workshop on lanternfish in the gulf of Oman, Muscat, Oman, 7–9* (Muscat: FAO).

Foote, G. (1980). Importance of the swimbladder in acoustic scattering by fish: A comparison of gadoid and mackerel target strengths. *J. Acoust. Soc Am.* 67, 2084–2089. doi: 10.1121/1.384452

Gjøsaeter, J., and Kawaguchi, K. (1980). A review of the world resources of mesopelagic fish. *FAO Fish. Tech. Pap.* 193, 123–134. doi: 10.1016/0010-0277(81)90009-3

Goodyear, R. H., Gibbs, R. H.Jr., Roper, C. F. E., Kleckner, R. C., and Sweeney, M. J. (1972). *Mediterranean Biological studies* (Washington DC: Smithsonian Institution), 2 355.

Greenlaw, F. (1977). Backscattering spectra of preserved zooplankton. *J. Acoust. Soc Am.* 62, 44–52. doi: 10.1121/1.381503

Grimaldo, E., Grimsmo, L., Alvarez, P., Herrmann, P., Tveit, G. M., Tiller, R., et al. (2020). Investigating the potential for a commercial fishery in the northeast Atlantic utilizing mesopelagic species. *ICES Mar. Sci.* 77 (7-8), 2541–2556. doi: 10.1093/icesjms/fsaa114

Guidi, L., Legendre, L., Reygondeau, G., Uitz, J., Stemmann, L., and Henson, S. A. (2015). A new look at ocean carbon remineralization for estimating deepwater sequestration. *Glob. Biogeochem. Cycles.* 29, 1044–1059. doi: 10.1002/2014GB005063

Hidalgo, M., and Browman, H. I. (2019). Developing the knowledge base needed to sustainably manage mesopelagic resources. *ICES Mar. Sci.* 76 (3), 609–615. doi: 10.1093/icesjms/fsz067

Horn, M. H. (1975). Swim-bladder state and structure in relation to behavior and mode of life in stromateoid fishes. *Fish. Bull.* 73 (1), 95–109.

Irigoien, X., Klevjer, T. A., Røstad, A., Martinez, U., Boyra, G., Acuña, J. L., et al. (2014). Large Mesopelagic fishes biomass and trophic efficiency in the open ocean. *Nat. Commun.* 5, 3271. doi: 10.1038/ncomms4271

Kaartvedt, S., Staby, A., and Aksnes, D. L. (2012). Efficient trawl avoidance by mesopelagic fishes causes large underestimation of their biomass. *Mar. Ecol. Prog. Ser.* 160, 103280. doi: 10.3354/meps09785

Kayama, M., and Ikeda, Y. (1975). Studies on the lipids of micronektonic fishes caught in sagami and suruga bays, with special reference to their wax esters. *Yukagaku (Lipid Chem.)* 24 (7), 435–440. doi: 10.5650/jos1956.24.435

Kayama, M., and Nevenzel, J. C. (1974). Wax-ester biosynthesis by midwater marine animals. *Mar. Biol.* 24, 279–285. doi: 10.1007/BF00396095

Kleckner, R. C., and Gibbs, R. H.Jr (1972). "Swimbladder structure of Mediterranean midwater fishes and a method of comparing swimbladder data with acoustic profiles," in *Mediterranean Biological studies, final report* (Washington, D. C: Smithsonian Institution).

Kloser, R. J., Ryan, T., Sakov, P., Williams, A., and Koslow, J. A. (2002). Species identification in deep water using multiple acoustic frequencies. *Can. J. Fish. Aquat. Sci.* 59 (6), 1065–1077. doi: 10.1139/f02-076

Kloser, R. J., Ryan, T. E., Young, J. W., and Lewis, M. E. (2009). Acoustic observations of micronekton fish on the scale of an ocean basin: Potential and challenges. *ICES J. Mar. Sci.* 66 (6), 998–1006. doi: 10.1093/icesjms/fsp077

Koslow, J. A., Kloser, R. J., and Williams, A. (1997). Pelagic biomass and community structure over the mid-continental slope off southeastern Australia based upon acoustic and midwater trawl sampling. *Mar. Ecol. Prog. Ser.* 146, 21–35. doi: 10.3354/meps146021

Kuhn, W., Ramel, A., Kuhn, H. J., and Marti, E. (1963). The filling mechanism of the swimbladder. generation of high gas pressures through hairpin countercurrent multiplication. *Experientia* 19, 497–511. doi: 10.1007/BF02150881

Lampitt, R. S., Achterberg, E. P., Anderson, T. R., Hughes, J. A., Iglesias-Rodriguez, M. D., Kelly-Gerreyn, B. A., et al. (2008). Ocean fertilization: A potential means of geoengineering? *Philos. Trans. A Math. Phys. Eng. Sci.* 366, 3919–3945. doi: 10.1098/rsta.2008.0139

Macdonald, A. G. (1975). *Physical aspects of deep sea biology*, 31.

Marshall, N. B. (1951). Bathypelagic fishes as sound scatterers in the ocean. *J. Mar. Res.* 10, 1–17.

Marshall, N. B. (1960). *Swimbladder structure of deep-sea fishes in relation to their systematics and biology*.

Marshall, N. B. (1979). *Developments in deep-sea biology* (Poole, Dorset: Blandford Press), 566.

Maynard, S. D. (1982). "Aspects of the biology of mesopelagic fishes of the genus cyclothone (Pisces:Gonostomatidae)," in *Hawaiian Waters* (Univ. Hawaii), 257.

McKelvie, D. S. (1989). Latitudinal variation in aspects of the biology of *Cyclothone braueri* and *C. microdon* (Pisces: Gonostomatidae) in the eastern north Atlantic ocean. *Mar. Biol.* 102, 413–424. doi: 10.1007/BF00428494

Meillat, M. (2012). Essais du chalut mésopélagos pour le programme MYCTO 3D-MAP de l'IRD, à bord du Marion dufresne. Du 10 au 21 août 2012. IFREMERRapport mission Marion DufresneRBE/STH/LTH 2012-05.

Mikami, H., Mukai, T., and Iida, K. (2000). Measurements of density and sound-speed contrasts for estimating krill target strength using theoretical scattering models. *Nippon Suisan Gakkaishi* 66, 682–689. doi: 10.2331/suisan.66.682

Miya, M., and Nemoto, T. (1986). "Reproduction, growth and vertical distribution of the mesopelagic fish *Cyclothone pseudopallida* (family gonostomatidae)," in *Indo-pacific fish biology: proceedings of the second international conference on indo-pacific fishes*. Eds. T. Uyeno, R. Arai, T. Taniuchi and K. Matsuura (Japan, Tokyo: Ichthyological Society), 830–837.

Miya, M., and Nemoto, T. (1991). Comparative life histories of the meso-and bathypelagic fishes of the genus *Cyclothone* (Pisces: Gonostomatidae) in sagami bay, central japan. deep Sea res. *Part I Oceanogr. Res. Pap.* 38 (1), 67–89. doi: 10.1016/0198-0149(91)90055-K

Neighbors, M. A. (1988). Triacylglycerols and wax esters in the lipids of deep midwater teleost fishes of the southern California bight. *Mar. Biol.* 98, 15–22. doi: 10.1007/BF00392654

Neighbors, M. A. (1992). Occurrence of inflated swimbladders in five species of lanternfishes (family myctophidae) from waters off southern California. *Mar. Biol.* 114, 355–363. doi: 10.1007/BF00350026

Neighbors, M. A., and Nafpaktitis, B. G. (1982). Lipid compositions, water contents, swimbladder morphologies and buoyancies of nineteen species of midwater fishes (18 myctophids and 1 neoscopelid). *Mar. Biol.* 66, 207–215. doi: 10.1007/BF00397024

Nelson, J. S., Grande, T. C., and Wilson, M. V. H. (2016). *Fishes of the world*.

Nevenzel, J. C., and Menon, N. K. (1980). Lipids of midwater marine fish: Family gonostomatidae. *Comp. Biochem. Physiol.* 6511, 351–355. doi: 10.1016/0305-0491(80)90025-5

Olivar, M. P., Bernal, A., Molí, B., Peña, M., Balbín, R., Castellón, A., et al. (2012). Vertical distribution, diversity and assemblages of mesopelagic fishes in the western Mediterranean. *Deep Sea Res. Part I Oceanogr. Res. Pap.* 62, 53–69. doi: 10.1016/j.dsr.2011.12.014

Olivar, M. P., Castellón, A., Sabatés, A., Sarmiento-Lezcano, A. N., and Bernal, A. (2022). *Abundance of mesopelagic fish collected at different layers of the water column around the Iberian peninsula* (PANGAEA). doi: 10.1594/PANGAEA.947631

Olivar, M. P., Contreras, T., Hulley, P. A., Emelianov, M., López-Pérez, C., Tuset, V., et al. (2018). Variation in the diel vertical distributions of larvae and transforming stages of oceanic fishes across the tropical and equatorial Atlantic. *Prog. Oceanogr.* 160, 83–100. doi: 10.1016/j.pocean.2017.12.005

Olivar, M. P., Hulley, P. A., Castellón, A., Emelianov, M., López, C., Tuset, V. M., et al. (2017). Mesopelagic fishes across the tropical and equatorial Atlantic: Biogeographical and vertical patterns. *Prog. Oceanogr.* 151, 116–137. doi: 10.1016/j.pocean.2016.12.001

Ona, E. (1990). Physiological factors causing natural variations in acoustic target strength of fish. *J. Mar. Biol. Assoc. UK.* 70, 107–127. doi: 10.1017/S002531540003424X

Ona, E. (1999). Methodology for target strength measurements. *ICES Coop. Res. Rep.* 235, 65. doi: 10.17895/ices.pub.5367

Osse, J. W. M., and van den Boogaart, J. G. (2004). "Allometric growth in fish larvae: timing and function," in *The development of form and function in fishes and the question of larval adaptation*, 167–194.

Peña, M. (2018). Robust clustering methodology for multi-frequency acoustic data: A review of standardization, initialization and cluster geometry. *Fisheries Res.* 200, 49–60. doi: 10.1016/j.fishres.2017.12.013

Peña, M. (2019). Mesopelagic fish avoidance from the vessel dynamic positioning system. *ICES J. Mar. Sci.* 76, 734–742. doi: 10.1093/icesjms/fsy157

Peña, M., Cabrera-Gámez, J., and Domínguez-Brito, A. C. (2020). Multi-frequency and light-avoiding characteristics of deep acoustic layers in the north Atlantic. *Mar. Environ. Res.* 154, 104842. doi: 10.1016/j.marenvres.2019.104842

Peña, M., and Calise, L. (2016). Use of SDWBA predictions for acoustic volume backscattering and the self-organizing map to discern frequencies identifying *Meganyctiphanes norvegica* from mesopelagic fish species. *Deep Sea Res. Part I Oceanogr. Res. Pap.* 110, 50–64. doi: 10.1016/j.dsr.2016.01.006

Peña, M., Andrès, L., and Quirós, R. G. (2023a). Target strength of Cyclothone species with fat-filled swimbladers. *J. Mar. Syst.*, 103884. doi: 10.1016/j.jmarsys.2023.103884

Peña, M., Moya, M., Carbonell, A., and Gonzalez-Quiros, R. (2023b). Vertical distribution and acoustic characteristics of deep water micronektonic crustacean in the Bay of BiscayMarine Environmental Research.

Peña, M., Munuera-Fernandez, I., Nogueira, E., and González-Quirós, R. (2021). First recording of a bathypelagic deep scattering layer in the bay of Biscay. *Progr. Oceanogr.* 198, 102669. doi: 10.1016/j.pocean.2021.102669

Peña, M., Olivar, M. P., Balbín, R., López-Jurado, J. L., Iglesias, M., and Miquel, J. (2014). Acoustic detection of mesopelagic fishes in scattering layers of the Balearic Sea (western Mediterranean). *Can. J. Fish. Aquat. Sci.* 71 (8), 1186–1197. doi: 10.1139/cjfas-2013-0331

Proud, R., Handegard, N. O., Kloser, R. J., Cox, M. J., and Brierley, A. S. (2019). From siphonophores to deep scattering layers : Uncertainty ranges for the estimation of global mesopelagic fish biomass. *ICES J. Mar. Sci.* 76, 718–733. doi: 10.1093/icesjms/fsy037

QGIS Development Team. (2022). *QGIS geographic information system* (Open Source Geospatial Foundation). Available at: https://www.qgis.org/es/site/.

R Core Team. (2022). *R: A language and environment for statistical computing*. Available at: https://www.r-project.org/.

Roe, H. S. J., and Badcock, J. (1984). The diel migrations and distributions within a mesopelagic community in the north East atlantic. 5. vertical migrations and feeding of fish. *Prog. Oceanogr.* 13 (3), 389–424. doi: 10.1016/0079-6611(84)90014-4

Sarmiento-Lezcano, A. N., Olivar, M. P., Caballero, M. J., Couret, M., Castellón, A., Hernández-León, S., et al. (2023). *Standard length, weight, body mass-density and swimbladder measurements data of cyclothone species from the IDEADOS, BATHYPELAGIC and SUMMER cruises in northeast Atlantic ocean and Mediterranean Sea* (PANGAEA). doi: 10.1594/PANGAEA.95494

Sarmiento-Lezcano, A. N., Olivar, M. P., Peña, M., Landeira, J. M., Armengol, L., Medina-Suárez, I., et al. (2022). Carbon remineralization by small mesopelagic and bathypelagic stomiiforms in the northeast Atlantic ocean. *Progr. Oceanogr.* 203, 102787. doi: 10.1016/j.pocean.2022.102787

Schaber, M., Gastauer, S., Cisewski, B., Hielscher, N., Peña, M., Sakinan, S., et al. (2022). Extensive oceanic mesopelagic habitat use of a migratory coastal and continental shark species. *Sci. Rep.* 12 (1), 1–14. doi: 10.1038/s41598-022-05989-z

Schneider, C. A., Rasband, W. S., and Eliceiri, K. W. (2012). NIH Image to ImageJ: 25 years of image analysis. *Nat. Methods* 9 (7), 671–675. doi: 10.1038/nmeth.2089

Scoulding, B., Chu, D., Ona, E., and Fernandes, P. G. (2015). Target strengths of two abundant mesopelagic fish species. *J. Acoust. Soc Am.* 137, 989–1000. doi: 10.1121/1.4906177

Simmonds, J., and MacLennan, D. (2005). *Underwater sound. fisheries acoustics theory and practice. 2nd edn* (Oxford, England: Blackwall Science).

Sobradillo, B., Boyra, G., Martinez, U., Carrera, P., Peña, M., and Irigoien, X. (2019). Target strength and swimbladder morphology of mueller's pearlside (*Maurolicus muelleri*). *Sci. Rep.* 9 (1), 17311. doi: 10.1038/s41598-019-53819-6

Stanton, T. K., Chu, D., and Wiebe, P. H. (1996). Acoustic scattering characteristics of several zooplankton groups. *ICES J. Mar. Sci.* 53, 289–295. doi: 10.1006/jmsc.1996.0037

Stickney, D. G., and Torres, J. J. (1989). Proximate composition and energy content of mesopelagic fishes from the eastern gulf of Mexico. *Mar. Biol.* 103, 13–24. doi: 10.1007/BF00391060

Strasberg, M. (1953). The pulsation frequency of non-spherical gas bubbles in liquids. *J. Acoust. Soc Am.* 25, 536–537. doi: 10.1121/1.1907076

Taylor, F. H. (1951). "Deductions concerning the air bladder and the specific gravity of fishes," in *Bulletin of the bureau of fisheries* (US Government Printing Office).

Taylor, F. H. C. (1968). The relationship of midwater trawl catches to sound scattering layers of the coast of northern British Columbia. *Fish. Res. Board Canada* 25, 457–472. doi: 10.1139/f68-040

Theilacker, G. H. (1980). Changes in body measurements of larval northern anchovy, *Engraulix mordax*, and other fishes due to handling and preservation. *Fish. Bull.* 78, 685–692.

Thompson, S. E., and Kenchington, T. J. (2017). Distribution and diet of Cyclothone microdon (Gonostomatidae) in a submarine canyon. *J. Mar. Biolog. Assoc. U.K.* 97 (8), 1573–1580.

Wiebe, P. H., Morton, A. W., Bradley, A. M., Backus, R. H., Craddock, J. E., Barber, V., et al. (1985). New development in the MOCNESS, an apparatus for sampling zooplankton and micronekton. *Mar. Biol.* 87, 313–323. doi: 10.1007/BF00397811

Yasuma, H., Sawada, K., Ohshima, T., Miyashita, K., and Aoki, I. (2003). Target strength of mesopelagic lanternfishes (family myctophidae) based on swimbladder morphology. *ICES J. Mar. Sci.* 60 (3), 584–591. doi: 10.1016/S1054-3139(03)00058-4

Yasuma, H., Sawada, K., Takao, Y., Miyashita, K., and Aoki, I. (2010). Swimbladder condition and target strength of myctophid fish in the temperate zone of the Northwest pacific. *ICES J. Mar. Sci.* 67, 135–144. doi: 10.1093/icesjms/fsp218

Yasuma, H., Takao, Y., Sawada, K., Miyashita, K., and Aoki, I. (2006). Target strength of the lanternfish, *Stenobrachius leucopsarus* (family myctophidae), a fish without an airbladder, measured in the Bering Sea. *ICES J. Mar. Sci.* 63, 683–692. doi: 10.1016/j.icesjms.2005.02.016

Yasuma, H., and Yamamura, O. (2010). "Second micronekton inter-calibration experiment, MIE-2. comparison between acoustic estimates," in *PICES scientific report no. 38*. Eds. E. Pakhomov and O. Yamamura. (Sidney, BC: Citeseer).